SOLAR CORONA EXPLORER

A Mission for the Physical Diagnosis of the SOLAR CORONA

SCIENCE WORKING GROUP REPORT
JULY 1981

SOLAR CORONA EXPLORER

A MISSION FOR THE

PHYSICAL DIAGNOSIS

OF THE SOLAR CORONA

PREFACE

This document has been prepared by the Science Working Group for the Solar Corona Explorer (SCE) under the chairmanship of Frank Q. Orrall. Thanks are due to the committee for the hard work they put into the effort of defining this important mission. The committee was also aided considerably by helpful discussions with Dr. David M. Rust and Dr. Edward N. Frazier.

Frank Q. Orrall, Chairman

Robert D. Chapman, Study Scientist

David H. Suddeth, Study Manager

Committee

Aaron Barnes
Leonard F. Burlaga
Stephen W. Kahler
Richard H. Munro
Frank Q. Orrall
Gerald W. Pneuman
Neil R. Sheeley
Arthur B.C. Walker
George L. Withbroe

Ex Officio

J. David Bohlin
George P. Newton
Robert D. Chapman
David H. Suddeth

I. INTRODUCTION

The Solar Corona Explorer Program is a quantitative, coordinated study of the corona and of the physical processes that form it, maintain it, and cause it to give rise to the expanding plasma of interplanetary space. It is now well recognized that many basic physical problems of the inner corona cannot be decoupled from those of the extended corona, solar wind and interplanetary medium. The Solar Corona Explorer will, for the first time, investigate the structure, dynamics and evolution of the corona, globally and in the required physical detail, to study the close coupling between the inner corona and the heliosphere. The objectives of the investigation are:

(a) to understand the corona as the source of the varying interplanetary plasma and of the varying solar X-ray and Extreme Ultraviolet fluxes;

(b) to develop the capability to model the corona with sufficient precision to forecast the Earth's variable environment in space, on time scales from weeks to years;

(c) to develop an understanding of the physical processes that determine the dynamics and physical state of the coronal plasma, particularly acceleration processes--processes that have broad astrophysical interest; and,

(d) to develop insight and test theory on the Sun applicable to stellar coronae and winds, and in particular, to understand why cool stars put such a large fraction of their energy into X-rays.

Interplanetary Plasma Physics and Coronal Physics have both reached a stage where many basic problems can only be solved by treating them as a single system. Skylab gave coronal physics a strong thrust, and it is reaching a plateau of understanding from which it can foresee the new observations needed to spur the next climb. Recent developments in stellar physics, especially the discovery that stars are far stronger

emitters of X-rays than predicted, have greatly stimulated interest in stellar coronal winds and magnetic fields. To better understand those phenomena in other stars, we must study our nearest star, the Sun. Solar coronal physics must continue to provide the guidance and testing ground for this work, but to do so, a far deeper understanding of coronal processes is required. This can be supplied by the Solar Corona Explorer Program.

In addition, it is timely and important to try to forecast the variable local environment of the Earth in space. That this environment profoundly influences the magnetosphere, ionosphere and upper atmosphere is of course certain, and the Origin of Plasmas in the Earth's Neighborhood (OPEN) mission is an intensive study of this interaction. Whether it exerts an important influence on the lower atmosphere is a subject of spirited debate. The slowly varying corona, and transient coronal activity, together largely determine the near-Earth magnetic field, the "field" of plasma properties, and the most energetic and variable portion of the radiation field. The modeling effort of the Solar Corona Explorer can be viewed as a timely and realistic effort to forecast the contribution of the slowly varying component of the corona to the near-Earth environment.

One major obstacle to a quantitative understanding of the solar and stellar coronae is the fact that the mechanisms that heat and accelerate coronal plasma are not known. Therefore, the crucial terms in both the momentum and energy equations that govern flow and structure can at best be characterized using plausible physical arguments. A number of promising mechanisms have been explored by theory--especially those evoking the deposition of wave energy and momentum--but no direct observation of their operation has been achieved: A necessary fundamental task of SCE will be to identify the physical processes that deposit both energy and momentum in the corona and solar wind flow, and to set new and forceful constraints on possible theories. One indirect but well defined approach will be to compare increasingly sophisticated models with direct observations of physical properties of the solar wind in the inner corona (i.e., geometry, density, pressure and flow velocity as functions of radial distance), so that the local deposition of heat and momentum can be inferred. In particular, velocity determination as a function of radial distance combined with diagnostic observations of the coronal base, is a new and essential capability of the SCE.

A second major study area is the interaction of the coronal plasma with the solar magnetic field. Large scale magnetic fields on the Sun tend to have insufficient tension to withstand the dynamic forces of the expanding corona which draw them out to interplanetary distances. It is along these "open" field lines (that originate from a limited fraction of the solar surface) that plasma escapes into interplanetary space. Stronger, smaller scale fields may resist these forces and remain for a time "closed." Closed field regions are usually formed by magnetic flux that has more recently emerged from below the photosphere. The plasma on closed field lines has a higher density than that on open lines, and probably also a higher temperature. As a consequence, closed regions give rise to most of the corona's XUV and X-ray emission. Thus, the interaction of the magnetic field with the coronal plasma produces the changing short wavelength brightness of the Sun's outer atmosphere. Yet to the present time, quantitative modeling of this interaction has been achieved only for the simplest geometry. The SCE will obtain the essential plasma data for both qualitative and quantitative studies of this interaction. Both of these examples illustrate the need for both morphological and diagnostic data, combined with numerical modeling, which is typical of many coronal problems.

Minimum Elements of the Program

The minimum elements for achieving the objectives of the program are:

(1) A 3-year mission launched as close as possible to the minimum of the sunspot cycle when the corona and interplanetary medium are at their simplest, with large open magnetic field regions at the poles. Three years is the significant fraction of a sunspot cycle needed to observe the slow persistent evolution of the large scale corona.

(2) A carefully coordinated instrument package capable of measuring plasma properties (e.g. electron density and temperature), velocity fields, magnetic fields, and morphology in the

transition region and corona out to at least 10 solar radii. Because these instruments must observe from the ultraviolet to the X-ray spectral regions, the package must be flown in space, and because of element (1) above, the spacecraft should be a free flier. A possible instrument package contains:

(a) A White Light Coronagraph (WLC) to measure the electron density and the evolving form of the corona from 1.5 to 10 solar radii, to record transient events, and permit inference to global magnetic structure from density measurements.

(b) A Soft X-Ray Imaging Telescope (SXT) to show the evolving form of the corona below 1.5 solar radii; to provide plasma temperatures and pressure, especially within closed field regions; and, to record the coronal manifestations of newly emerged magnetic flux.

(c) A Resonance Line Coronagraph (RLC) to measure coronal plasma properties and systematic velocities as a function of height from 1.2 to 8 solar radii above the limb.

(d) An EUV Diagnostic Spectrometer (EDS) to measure systematic velocities and plasma properties of the transition region and corona below approximately 1.3 solar radii in order to define the varying lower boundary of the inner corona and solar wind.

(3) Full disk measurement of the longitudinal component of the photospheric magnetic field with a spatial resolution of a few arcseconds and a precision of about 1 gauss, nominally daily, is essential to the major aims of the mission. (The SWG found many strong arguments for placing a Magnetograph on the spacecraft as a fifth instrument, but since ground-based observations with existing instruments could probably provide the bare minimum requirements for some major aims of the mission, we have not given it as high a priority. This recommendation should be reviewed pending cost and design studies of the impact of adding a fifth instrument.)

(4) A coordinated program of ground-based solar observations to complement those from the spacecraft.

(5) A vigorous program of interpretation and modeling during and after the mission, must be supported and considered an integral part of the mission if the concrete aims of this program are to be achieved.

Recommended Schedule

Launch of the SCE in 1987 is timely. The mission would then operate from near the predicted sunspot minimum through the rise toward maximum, and would overlap with the OPEN program (a mission dedicated to the Origin of Plasmas in the Earth's Neighborhood) and the ISPM (the International Solar Polar Mission). The Solar Corona Explorer, standing alone, is a strong self-contained, coherent mission with clear, fundamental and realistic objectives. However, if it were in orbit simultaneously with either OPEN, ISPM, or both, it would offer a unique opportunity of unprecedented value for studying that complex system comprising the Sun, the Earth and the interplanetary medium. The ISPM and IPL (a component of OPEN) will make in situ observations of the interplanetary plasma both out of and in the ecliptic plane respectively. These would provide the firmest interplanetary constraints on models of coronal expansion that we can reasonably hope for in the near future. One of the ISPM spacecraft bears a white light coronagraph and a soft X-ray imaging telescope, which together with similar instruments on the SCE can make stereo observations of coronal structure and transient events. These stereo observations can be used for a reconstruction of the three-dimensional form of coronal structures.

The recommended mission launch and duration is shown in Figure I-1 together with current estimates for OPEN and ISPM, with projected times of sunspot minimum and maximum.

Scientific background and more detailed scientific objectives of the SCE program are given in Chapter II, and details of implementation in Chapter III.

II. SCIENTIFIC OBJECTIVES

1. THE STRUCTURE AND EVOLUTION OF THE SUN'S OUTER ATMOSPHERE

Before we define the approaches required to solve the outstanding problems in coronal physics, we will take a brief look at the current state of the subject.

Coronal Holes

Figure II-1, a composite of a Skylab soft X-ray image and a ground-based white-light image obtained during the June 30, 1973 total eclipse, illustrates the general features of the Sun's outer atmosphere. In the X-ray image, many small bright points and several larger active regions are visible against a background of fainter emission which itself has some structure. The background is interrupted by a rift of greatly reduced intensity that extends from the north pole to a point well into the Sun's southern hemisphere. Along the edges of this rift, curvilinear emission features bend outward and extend upward into the outer corona. Here they merge with the surfaces of white-light streamers, and thereby define the boundary of a very large wedge-shaped hole in the Sun's corona. Most of the white-light emission originates in such helmet streamers that stretch increasingly radially from their bright loop-shaped bases as they reach farther from the Sun. Finally, relatively faint, curvilinear plumes extend outward from the solar polar limb, and, unlike the helmet streamers, become invisible beyond a few solar radii from the Sun's center.

All of these coronal structures reflect characteristics of the Sun's magnetic fields. The bright points and active regions are volumes of dense, high-temperature plasma that is confined by closed, strong magnetic fields. Coronal holes are volumes of relatively rarified, low-temperature plasma that is escaping outward along open magnetic field lines to produce high-speed streams in the solar wind. Coronal streamers indicate the tops of closed magnetic loops that are stretched outward by the forces of the expanding plasma. The resemblance of polar plumes to

the field lines of a uniformly magnetized sphere has long suggested that these features trace the outward extension of field lines from the Sun's polar caps. However, the flight observations suggest that such plume configurations are really emission from relatively thin anterior and posterior boundaries of the polar coronal holes (which also map out field lines).

There are two difficulties that prevent us from deriving information about coronal structure from observations of the Sun's photospheric magnetic field. First, we do not have a complete understanding of the plasma forces that perturb the coronal field from its potential-field configuration, and we cannot solve the hydromagnetic problem posed by the corona except in the simplest geometries. Second, our observations of the photospheric magnetic field are necessarily incomplete, since we need the global flux distribution, but measure only the line-of-sight component. As a result we never have a direct knowledge of the polar fields where the lines of force are roughly perpendicular to the line of sight and, because of temporal changes that occur during a 27-day synodic solar rotation period, we cannot even obtain a true representation of the global field at low latitudes.

Despite these difficulties, we have increased our empirical understanding of the plasma-field interaction considerably by comparing both direct coronal observations, such as X-ray images and white-light coronal images, and indirect coronal observations, such as He I 10830 Å and He II 304 Å images, with photospheric magnetograms. We have learned that coronal holes form in large-scale magnetic regions of locally-unbalanced flux whose field lines are, therefore, presumably open, that is, that connect with the interplanetary field. In the absence of new sources of flux (i.e. sunspot groups), large-scale magnetic field strengths gradually decrease with time and the coronal holes lose contrast relative to their surroundings as observed in X-ray and helium images and shrink in size. This process is common near sunspot minimum. However, holes that have become dormant are greatly strengthened when suitably-oriented bipolar magnetic regions emerge in their vicinity. Such coronal hole rejuvenations were common during the rising phase of the present sunspot cycle. Coronal holes share the evolutionary behavior of the fields in

which they are located, and, in particular seem to undergo differential rotation. Equatorial holes recur at 27-day intervals, while small, high-latitude holes recur at longer intervals, and large high-latitude holes gradually become sheared into nearly east-west oriented structures. This latitude dependence was not fully appreciated until high-latitude holes became common during the rising phase of the present sunspot cycle. Finally, near sunspot minimum when the Sun's polar fields are strong, there is a tendency for coronal holes to be generated, or rejuvenated, by that half of a bipolar magnetic region whose polarity agrees with the sign of the polar field in that hemisphere (following polarity during the declining phase of the cycle and leading polarity during the rising phase). This tendency disappears near sunspot maximum as the polar fields vanish.

Coronal holes are useful not only to study the Sun's large-scale magnetic structure, but also to forecast the occurrence of high-speed solar wind streams and their associated geomagnetic disturbances. In fact, this forecasting capability has provided considerable motivation for coronal research in recent years. Figure II-2 summarizes our observational knowledge of the correlation between the central-meridian-passage dates (plus 3 days to allow for an average Sun-Earth transit time) of coronal holes within 40° of the Sun's equator, the daily average solar wind bulk speed at Earth, and the daily geomagnetic activity index C9 during the 7-year interval 1973-1979. For reference, the inferred interplanetary magnetic field (IMF) polarity is shown on the left and a 27-day average sunspot number is shown in the narrow strip on the extreme right. The coding and other details are given in the figure caption.

One conclusion from the data presented in Figure II-2 is that, although coronal holes were present throughout this 7-year interval, they were not always associated with high-speed solar wind streams at Earth. A detailed study of individual holes indicates that there is a correlation between the solar latitude of the hole and terrestrial effects.

Thus we see that both space-based and ground-based observations have greatly improved our empirical knowledge of the structure and evolution of the Sun's outer atmosphere. Nevertheless, fundamental questions remain even for a qualitative understanding.

Weak or Dormant Coronal Holes

We have noted that ground-based He I images at 10830 Å and a few rocket-based X-ray images during the past sunspot minimum have shown the presence of weak coronal holes. The fact that coronal holes can have a range of contrast relative to their surroundings raises several important questions. If holes can be very weak and still produce high-speed streams, as they often did in 1976 during the last sunspot minimum, then the hole must be determined by something more basic than its contrast on an X-ray or helium image. This conclusion, together with the fact that holes come and go within a slowly-evolving, long-term sector pattern, gives rise to the concept of dormant holes which may be simply large-scale regions of weak, but unipolar, magnetic fields. If dormant holes do exist and indicate the places where rejuvenated holes can be created by the emergence of new bipolar magnetic regions, then one should be able to identify probable locations of new holes by keeping track of the large-scale fields that are associated with the dormant holes. It is clearly important to calculate the future evolution of the large-scale photospheric magnetic fields as they are transported by random-walk diffusion and differential rotation.

The Solar Corona Explorer with the capability for obtaining soft X-ray images and white-light coronal images would address many of these questions regarding coronal holes. Of course, supporting full-disk photospheric magnetograms will be essential. While such magnetograms might be obtained from ground-based observatories, at present there is only one instrument (at Kitt Peak National Observatory) with sufficient spatial resolution (3 arc sec), and the availability and quality of its observations are subject to the whims of the atmospheric weather and seeing conditions. An onboard magnetograph that is dedicated to the coronal mission could make an invaluable contribution toward the solution of the problems raised above. In particular, the consistent sensitivity and image quality that would be obtained from space will be especially important for studying the weak, fragmented flux distributions that are associated with weak coronal holes.

Coronal Structure and High Speed Wind Streams

Another area in which the Solar Corona Explorer can make an important contribution is the relation between coronal structure and high-speed solar wind streams. As we have noted in Figure II-2, coronal holes do not always produce high-speed streams at Earth. Past observations with ground-based He I 10830 Å images suggest that the reason for this lack of correlation is associated with the latitude of the holes relative to the heliographic latitude of Earth. Yet the variation in the latitude of coronal holes is several tens of degrees where as the seasonal variation of the Earth's heliographic latitude is only $\pm$ 7.25°. This fact raises the question of how the relatively small $\pm$ 7.25° variation could produce the relatively large seasonal variation in the correlation between holes and high-speed streams at Earth that we found during 1976-1979 (Figure II-2).

Figure II-4 provides a possible answer to this question, and emphasizes the importance of obtaining white-light coronal observations in the study of the hole-stream correlation. The figure shows a sequence of white-light coronal images obtained from the P78-1 Air Force Satellite during three consecutive limb passages of a larger, southern-hemisphere coronal hole. The hole is visible alternately in the south-east, south-west, and south-east quandrants as a streamer-free region ranging from approximately 65° latitude on one side of the south pole to a position near the equator on the other side. The Bartels display in Figure II-2 showed that this negative-polarity coronal hole was associated with a 500-km/sec solar wind stream at Earth despite the fact that the northern-most boundary of the hole reached only 15° S latitude at the chromospheric level shown in the He I 10830 Å images. The coronal images suggest that the good correlation between the hole and the solar wind speed at Earth was due to the fact that the hole's boundary expanded non-radially into the corona where its associated solar wind stream was directed toward the Earth. Thus, such white-light coronal images together with soft X-ray images such as Figure II-3, will provide a direct physical test of the latitude-dependent correlations such as the one shown in Figure II-2. As described in detail elsewhere, this information provides an invaluable complement to the observations that will be obtained from high heliographic latitudes by the ISPM.

Other Coronal Hole Studies

During the Skylab mission investigators were able to observe the birth of only one coronal hole, and in that case the X-ray observations were obtained with poor time resolution. Figure II-5 shows three X-ray images taken during the birth of a coronal hole. The birth occurred in a large unipolar hole of relatively low X-ray intensity, but the detailed structural changes could not be followed closely in time. A mission with several years of observations will be able to observe a number of births.

The way in which coronal hole areas change was explored statistically using Skylab data. Most changes in coronal hole areas could be explained by large scale changes of characteristic length more than 9×10^4 km at the boundaries. The time scales and mechanisms of these boundary changes have not been studied in detail. It was also found that coronal X-ray transients outside active regions tended to occur preferentially on neutral lines associated with the boundaries of coronal holes. The detailed relationship between an X-ray coronal transient and any associated coronal hole boundary change has yet to be investigated. These studies can fruitfully be explored with the high resolution X-ray imaging on the SCE.

Magnetic Reconnection

Even though the corona is quite stable during solar minimum, slow changes are nevertheless always taking place as is evident by comparing images from rotation to rotation. The changes seem to reflect evolution in the surface field configuration and, apparently, occur in such a way as to maintain the coronal magnetic field as close to potential as possible. Evidence for this statement comes from calculations of global coronal magnetic field structure based upon both the upward extrapolations of the observed line-of-sight photospheric field measurements, and the assumptions that the field in the corona is potential up to a prescribed height and radial beyond--simulating the action of the solar wind. These extrapolations show good qualitative agreement between calculated open field lines and the locations of coronal holes as seen in soft X-rays

and also predict quite well the locations of high speed streams as observed at the Earth. The apparent fact that the coronal field remains approximately potential despite constant motions of the photospheric footpoints is surprising in view of the enormous electrical conductivity of the corona. One might expect the field lines to be quite tangled and twisted but considerable potential-like order is observed as one can see in Figure II-6. Evidently a process of field line reconnection takes place to maintain the nearby potential field. Figure II-7 shows schematically how this process might occur topologically as new flux emerges on the Sun to interact with its surroundings. Several Skylab observations have been presented as evidence of reconnection, but magnetic fields have not yet been directly measured in the corona. There are always line-of-sight ambiguities in the positions of X-ray emitting features, and other interpretations are consistent with the data. The best possible observations bearing on this question, are stereo images (from SCE and ISPM) to resolve the line-of-sight ambiguities and good magnetograms to establish the magnetic field configuration of the region. These data can then be used to establish locations and time scales of reconnection.

Large-scale coronal magnetic field reconnections presumably occur continually at the boundaries of the polar coronal holes as the low-latitude footpoints of loops from the edges of the holes are separated from their high-latitude footpoints by differential rotation. Also, such reconnections are presumed to occur during rapid changes in the boundaries of coronal holes and in the formation of some short-lived coronal holes that are associated with disappearing filaments and eruptive prominences. The occasional appearance of such phenomena in the Skylab X-ray images and in post-Skylab ground-based helium images suggest that both X-ray and white-light coronal images should be obtained at intervals of 10 minutes or less during these events.

Tomographic Observations of Coronal Structure

It is possible to determine the three-dimenstional structure of the corona from only one vantage point by using the Sun's rotation to present different perspective views to the observer. This method relies upon the assumption that the corona does not change significantly during the

temporal sequence of observations, usually about 7 to 10 days for a particular coronal feature to pass over the limb of the Sun in the case of coronagraphic observations. We know that features do change on time scales from tens of minutes to months, so this type of three-dimensional determination must contain inherent errors created by evolutionary processes. For many purposes nevertheless, it is reasonable and useful to assume the corona does not change.

The addition of another observational point, especially from over the solar pole, will eliminate the confusion between effects of temporal changes and the solar rotation. The passage of ISPM over the solar poles will probably occur after solar minimum. Many coronal streamers will still exist as equatorial structures in the simplified dipolar picture of the Sun near minimum, and hence will not as easily be studied by instruments in the ecliptic plane. Observations from two vantage points at large angular separation would reveal the true shape of these streamers. Similarly equatorial coronal holes seem to be elongated in the north-south direction and are often obscured by surrounding coronal streamers. The added data from ISPM would permit the true three-dimensional determination of the geometry of these holes. All of our estimates of the properties of coronal transients are dependent on assumptions of their geometry. That geometry cannot be uniquely determined from a single view. The combination of observations from orthogonal perspectives would give true trajectories and distinguish between competing geometric models. Finally, coronal observations from the ecliptic cannot continually monitor the corona that is obscured by the solar disk; the addition of polar views will greatly enhance our knowledge of the other 50 percent of the corona and its evolution between limb passages. Obviously the greatest use of this combined set of data will be the unambiguous production of the three-dimensional picture of the solar corona.

The tomographic process can be visualized in the following manner. In Figure II-8, the X-ray or white-light image of a target region T obtained with each telescope consists of an n x n spatial array of intensities. As the Sun rotates, the view of T from the SCE changes continuously, so views of T from significantly different angles can be

made. If the evolution of T is insignificant over the time period of the observations, the data can be used to reconstruct a three-dimensional matrix of X-ray brightness. With a total of N views from both ISPM and SCE the general algorithms used for tomography permit a total of m^3 points in the matrix when $m^3 \leq 3 (n \times n \times N)$. The SCE and ISPM data sets can be treated equally, i.e., equal numbers of images from each spacecraft are used in the reconstruction, or one of them (the ISPM data in this case) can be used to provide "boundary conditions" for the SCE data which would be of higher spatial resolution. In the latter case, the ISPM data would be used to resolve the inevitable ambiguities of the reconstruction program. These ambiguities have hampered past attempts to do tomographic reconstruction with the Skylab X-ray images.

2. IMPACT OF THE SOLAR CORONA EXPLORER ON STUDIES OF THE PHYSICS OF THE SOLAR WIND

The SCE will provide a unique opportunity to advance understanding of the acceleration of the solar wind, its morphology, and sources. As we discuss below, this advance will mainly come about through use of SCE observations in conjunction with those from other missions; however, in one important respect the SCE stands alone. The SCE will be the first mission to provide long-term, synoptic observations of temperature and flow velocity as a function of height, and the plasma properties of the base of the corona. These observations will greatly clarify the spatial dependence of the forces that drive the wind, thus definitively reducing the list of candidate mechanisms for solar wind acceleration and heating. By themselves, these observations could produce a quantum jump in our understanding of solar wind dynamics.

The impact of the SCE on solar wind physics will be much amplified if it overlaps with the ISPM and the OPEN Mission. According to present estimates, the two spacecrafts of the ISPM will be at high latitudes (one in the north, one in the south) in 1988-9; simultaneously the IPL of OPEN will be measuring the solar wind in the ecliptic plane near the orbit of Earth. The NASA spacecraft of the ISPM will carry instruments to view the corona in white light, ultraviolet and X-radiation. Analogous

instruments on the SCE will give ecliptic views in the same modes. As discussed elsewhere, observations from the two missions taken together will give stereoscopic and tomographic pictures of the corona, permitting the first truly three-dimensional synoptic study of coronal structure. In addition, the ISPM spacecraft at high latitudes and the IPL in the ecliptic will give direct measurements of the solar wind velocity parameters and magnetic field, and related quantities. These observations, in conjunction with ISPM and SCE coronal observations, will dramatically expand our knowledge of solar wind morphology and its relation to coronal structure. In particular, it should be possible to identify the sources of all types of solar wind flows and their magnetic fields. It will be possible to determine how these sources evolve with time and to study the effects of this evolution on the solar wind.

The high-latitude passage of ISPM will probably occur just after the minimum of the sunspot cycle. It is anticipated that the morphology of the heliosphere will be in some respects similar to that inferred from SKYLAB coronal observations, and interplanetary plasma and magnetic observations one cycle earlier. Thus we expect large polar coronal holes, possibly with extensions to low latitudes. During the SKYLAB period unusually fast, broad, long-lived solar wind streams were found in the ecliptic, and the source appeared to be at intermediate to low latitudes. IPL is likely to find similar streams in the ecliptic, and at high latitudes the ISPM spacecraft should be continually immersed in the fast stream from the polar hole. The interplanetary magnetic field is generally believed to be divided into two hemispheres of opposite polarity, separated by a warped current sheet which is roughly centered on the solar equatorial plane, but which passes well above and below ($\sim$15 to 20°) the equatorial plane. Thus a spacecraft in the ecliptic typically sees two or four sectors of opposite magnetic polarity during a solar rotation. In contrast, each ISPM spacecraft should see uniform magnetic polarity at high latitudes, inward toward the Sun in the north, outward in the south.

This general picture of solar-wind morphology, if confirmed by the ISPM, implies a unique opportunity for investigation of solar wind dynamics

with data from the ISPM. A major difficulty in this field has been that the interplanetary mixing of solar wind streams greatly distorts the effects of varying coronal conditions, so that ecliptic observations of the solar wind are particularly difficult to relate to a particular part of the corona. In contrast, stream mixing at high latitudes should be much weaker (unless the spatial structure of the corona itself varies especially rapidly at high latitudes). In this case it is more reasonable to consider high-latitude measurements of velocity, density, etc. in the context of steady-flow theories. This fact is a major advantage for the study of acceleration and heating, because much more sophisticated and realistic heating and acceleration mechanisms can be incorporated in steady-flow models than in time-dependent models.

Thus the ISPM and the SCE together represent the best opportunity for many years to come for making a combination of in situ and remote sensing measurements that have an important bearing on the question of solar wind acceleration and heating. This subject is of special scientific importance not only because the solar wind is the electrodynamic connecting link between the Sun and the rest of the solar system (including Earth), but also because the solar wind is the most easily studied example of a stellar wind, the main process by which most stars shed mass and angular momentum. Accordingly, it is especially important to have good coronal observations during the ISPM and OPEN/IPL. This need is partly supplied by coronal instrumentation on the ISPM itself. However, it is also imperative to have the simultaneous synoptic coronal measurements in the ecliptic that SCE will supply in order to determine the three-dimensional structure of the polar corona.

The resonance line coronagraph (RLC) on SCE is a particularly valuable instrument for studying solar wind acceleration and heating, because it gives the temperature and flow velocity as a function of distance between 1.2 to 8 R_o, which is precisely the region in which significant heating and acceleration of the solar wind is believed to take place. The ISPM payload does not include a RLC, and there are no plans for one on OPEN/IPL. The IPL will, however, make excellent measurements of the charge state composition of the solar wind as a

function of time. This composition is related to the temperature and density profiles in the corona, but it is not possible to uniquely determine the temperature and density profiles from these measurements alone. Given simultaneous temperature and density profiles from SCE, and measurements of the solar wind composition for IPL, it will be possible to construct self-consistent models relating all of these parameters. Together with measurements of the solar wind out of the ecliptic from ISPM, the IPL and SCE observations will give powerful constraints on the viability of theories of solar wind acceleration.

While SCE observations will contribute much to a better understanding of the solar wind in general, and of the OPEN/IPL measurements in particular, it is equally true that ISPM and OPEN/IPL will contribute significantly to a better understanding of the corona and to interpreting SCE observations. The interplanetary spacecraft will make direct observations of solar material and solar magnetic fields. Plasma elements in the solar wind carry an integral measurement of the temperature in the corona, as described above, and they also carry information about the physical conditions and chemical composition of material at the base of the corona.

Magnetic field measurements by ISPM and OPEN/IPL should be particularly valuable, because they provide a means of inferring the coronal magnetic field. The magnetic field is the dominant form of energy in the lower corona and it strongly influences the material there, yet there is presently no way to measure the coronal magnetic field directly. The interplanetary magnetic fields originate at the Sun, and they are directly related to coronal magnetic fields. Combining the local interplanetary magnetic field measurements with global measurements of the photospheric magnetic field will give a fairly accurate and comprehensive picture of the strength and topology of the coronal magnetic field as a function of time. In any case, these measurements, together with measurements of the density and temperature in the corona will put very strong constraints on coronal models.

IPL will measure the solar wind and interplanetary magnetic field continuously for five years, beginning in 1985 or 1986 according to present plans. Thus, it will be possible to directly study the evolution of the solar wind and magnetic field as a function of time from solar minimum to near solar maximum. Such measurements have been made before, but without a comprehensive set of data describing the corona and without complete composition measurements. With IPL and SCE it will be possible to study the evolution of plasmas and magnetic fields in the corona, their response to changing solar activity, and their effects on interplanetary conditions.

3. MODELING CORONAL STRUCTURE AND SOLAR WIND FLOW

Changes in the structure of the solar corona take place chiefly on two distinct time scales--one associated with solar activity, i.e., flares and eruptive prominences, and one due to changes associated with the solar cycle. The first is a time scale of hours whereas the latter changes occur over a period of months. Around sunspot minumum when activity is at its lowest, the corona assumes its most stable form, changing only very slowly from rotation to rotation. This is the best time to study basic coronal structure since, at this time, the corona has its simplest form; a simple dipole warped somewhat about the equator.

Plasma-Magnetic Field Interaction

Steady state coronal structure seems to be almost completely determined by the configuration of the large-scale magnetic fields of the Sun. Since the corona has an enormous electrical conductivity and since the coronal gas is almost completely ionized, the material is prohibited from crossing magnetic field lines but can move freely along them. Hence, in regions of the corona where the field is 'closed' (e.g., loops, arcades) the gas is bottled up in the inner corona. Where the field is 'open' on the other hand, expansion into interplanetary space, i.e., the solar wind, can take place freely. Thermal conduction acts in much the same way, taking place easily along open field lines. This means that, where the magnetic field is open, the hot corona can

lose energy both by outward thermal conduction and in the kinetic energy of the expansion (the energy carried by thermal conduction is all eventually converted into kinetic energy of the solar wind). As a result, one expects the temperature in open field regions to be somewhat lower than in closed regions where these losses cannot occur. This temperature difference produces a difference in scale height in the two regions resulting in a higher gas density in closed loops than on open field lines by a factor of about 3 to 100. This effect produces the characteristic structure of the corona seen during eclipse and with coronagraphs, X-ray instruments, etc. In soft X-rays this contrasting behavior is most striking and is manifest in the presence of dark 'coronal holes'.

In closed field regions the characteristic coronal structure is the streamer, consisting of closed loops near the Sun and open field lines outside and above. The open field lines are produced by the solar wind. The streamers are best seen during total eclipse and are well illustrated as the bright regions in Figure II-1. In the absence of electric currents, the magnetic fields of the corona would be potential and all field lines would be closed. However, the tendency for the corona to expand pulls closed fields outward into an open configuration where the fields are weak, thus, generating electric currents. Hence, close to the Sun where the fields are strong, they can contain the gas and remain closed but higher up the fields weaken and are pulled open. An exact solution of the Magnetohydrodynamic (MHD) equations for this particular type of gas-magnetic field interaction has been obtained for a particularly simple geometry and is shown in Figure II-9.

Little is known about the three-dimensional structure of streamers because of limitations in viewing them from different angles. For this reason, simultaneous coronagraph observations of these interesting structures from the solar poles and from the ecliptic would be invaluable in understanding the physical processes taking place. The same arguments hold for soft X-ray observations of streamers lower in the corona. If the minimum corona has the magnetic structure we expect, then the ecliptic view would be considerably more complex than the view from the pole. Polar observations of streamers might be difficult to interpret without simultaneous in-the-ecliptic views.

Coronal holes and coronal streamers provide two different but ideal structures for studying the complex interaction between the dynamic and static forces of the coronal plasma, and the magnetic field. The exact symmetrical MHD solution in Figure II-10 is one of the few such solutions that we possess. It has holes in the polar regions, and a single streamer encircling the equator. This approximates the corona in minimum, although in reality the neutral line at the equator may be warped, and the equatorial streamer fragmented. What makes the problem difficult is that the flow of plasma is greatly influenced by the geometry which is provided by the shape of the magnetic field; but the shape of the field depends on the flow. The X-ray and white-light instruments on the SCE can provide the detailed observations of the geometry needed to study the plasma-magnetic field interaction.

Coronal Heating and Acceleration

If the corona were not heated mechanically or non-thermally from below, its temperature would always be lower than that of the photosphere. The coronal gas would be mainly neutral, and the temperature would decline rapidly outward in accordance with the losses incurred by radiation and thermal conduction (here, the thermal conductivity would not be high as for an ionized gas but, would be that appropriate for neutral hydrogen). Under these conditions, expansion would not be required and the solar wind would not exist. So in a very direct sense, the solar wind is produced by coronal heating. Mechanically speaking, the wind is driven by the large pressure difference between the coronal base and the interstellar medium. The pressure difference is produced by heating which raises the temperature of the inner corona to over a million degrees, almost three orders of magnitude higher than the photospheric temperature. Thus, the corona is too hot to be static. The mechanism involved in heating the corona is not known, although heat deposited by the dissipation of waves generated by convective motions is currently the most popular explanation. However, the presence of waves in the inner corona has never been confirmed by observation. Another possibility for heating the corona is through Ohmic dissipation of electric currents produced either by the interaction of convection with

magnetic fields or by small-scale magnetic reconnection. This whole question of coronal heating could be clarified by high resolution observations of the inner corona and transition region. Again, solar minimum is ideal for these observations since there will be less confusion introduced by disturbances and heating effects due to flares and active region evolution.

Understanding coronal heating will clarify greatly our understanding of how the solar wind is accelerated in the inner corona. To date, solar wind theories specify the distribution of heat input in an ad hoc manner and, hence, the predictions of all these theories rest upon shaky foundations. Most assume the heat input takes place at a very low level (usually in the transition region) so that the wind equations can be integrated outward from there without specification of a heat input function. Theories such as these, however, predict solar wind speeds at 1 A.U. of about 300 km s^{-1}--over a factor of two lower than that observed in the highest speed streams. Furthermore, it can be shown that adding additional heat in the inner corona (below the critical point) does not solve the problem since it further reduces the predicted wind speed. Hence, some additional accelerating mechanism besides thermal pressure must be operating, such as Alfven waves or spicules, through direct momentum addition.

As a more concrete illustration, let F be the component of acceleration due to non-pressure forces whose source is unknown. Suppose we know the run of pressure and density as a function of radial distance, P(r) and $\rho(r)$ respectively, and the flow velocity at two heights (v_1 and v_2). A first integral of the momentum equation (in simple geometry) yields:

$$\frac{1}{2}\,(v_2^2 - v_1^2) + \int_{r_1}^{r_2} \frac{1}{\rho}\left(\frac{dp}{dr}\right) dr + GM_o\left(\frac{1}{r_1} - \frac{1}{r_2}\right) + \int_{r_1}^{r_2} F\,dr = 0$$

We can thus determine the mean acceleration due to the unknown force. Given in addition the temperature, the radiative losses can be calculated and the total energy deposition in the interval inferred. These are basic quantities needed to explore or constrain theories of coronal heating and acceleration. The SCE will be able to supply the necessary observations to infer these physical quantities. The Resonance Line

Spectrograph will measure the quantities v(r) and T(r), and the White Light Coronagraph will measure electron densities Ne(r) from which we can infer $\rho(r)$. Given the equation of state

$$P = 2nkT,$$

we can calculate pressure $\rho(r)$ from the measured n(r) and T(r). Thus, the only unknown in the first integral of the momentum equation is the force. We have given this illustration here to stress the importance of direct velocity measurements. In practice, the study of heating and acceleration is closely related to modeling, to which we now turn.

Modeling

By modeling, we mean the calculation (via a numerical model) of the time varying three-dimensional structure (density, temperature, velocity, magnetic field) of the steady state or slowly varying solar corona from its base out to the orbit of Earth. The necessary inputs to such a model are the photospheric magnetic field strength, the temperature and density as a function of latitude and longitude at some prescribed level in the lower corona, and knowledge of heat deposition and possible acceleration mechanisms. The output of such a model is to be compared with other observations of the inner corona as well as with spacecraft observations of the solar wind at 1 A.U. Such modeling efforts have previously been attempted with some limited success and are able to predict such qualitative features in the solar wind at 1 A.U. as the location of high speed streams. Even this agreement is a little surprising considering the crudity of the inputs to the model. The magnetic field model was a simple extrapolated potential field with a source surface beyond which the field was set radial, the density at the coronal base was obtained by a crude deconvolution of K-coronameter data (much better deconvolution methods now exist), estimated temperatures at the coronal base were used. Coronal heating above the base and accelerating mechanisms other than thermal pressure were neglected. Yet, the relative success of this modeling attempt with limited data and necessarily incomplete theory provides the guidance for designing a major advance in coronal modeling.

The SCE will provide a consistent, uninterrupted global data base, including synoptic global observations of the base of the corona with the EUV diagnostic spectrograph. Increasingly realistic heating and acceleration processes will be incorporated in the model based on the unique ability of the SCE to provide velocity and geometric data. Simultaneous interplanetary data from ISPM and IPL would provide tight constraints and tests on models and theory.

Coronal Rotation

The coronal magnetic field also has a strong influence upon the rotation of coronal material. Due to differential rotation of the photospheric layers, magnetic loops with footpoints rooted at different solar latitudes will experience differences in angular velocity from one footpoint to the other. If this difference were unopposed, the loops would after a few solar rotations be all oriented in the East-West direction. Although there is some indication of this in ground-based K-coronameter observations, the effect is not nearly as pronounced as one might expect from the observed photospheric differential rotation. Theory suggests however, that, in low β plasmas such as that in the lower corona, magnetic stresses are set up which tend to equalize the angular velocity along the loop to an average rate lying somewhere between the velocity of the two footpoints. Hence, differential rotation (in closed regions only) should tend to wash out as one proceeds to greater heights. Although there is some observational support for this conclusion from K-coronameter data, coronal rotation is still poorly understood and long-term observations from space are needed. In this connection, observations during solar minimum should be the most illuminating since the basic rotational process will be less interrupted by flares and transients.

4. DYNAMIC CORONAL PHENOMENA

So far we have emphasized steady state and slowly changing aspects of the corona, since these can be uniquely exploited by the SCE because of its proposed launch at solar minimum. Nevertheless, the corona is not completely inactive even during this period. Flares, eruptive

prominences, coronal transients and other types of solar activity still occur at this time although certainly with less frequency. This is not particularly a disadvantage in observing solar activity as it may, in some cases relieve confusion. With the rise to maximum later in the mission, active phenomena will become common.

Probably the most spectacular and persistent features associated with the classic large two-ribbon solar flares are the so-called flare loops or 'post-flare' loops. These loop systems begin at the very onset of the flare and are observed to rise upward slowly into the corona. The velocity of ascent decreases with height from about 10 to 20 km s^{-1} when they are finally seen in soft X-rays at great heights of sometimes over 100,000 km. The system does not appear to consist of single rising loops but, rather of newly formed or activated stationary loops appearing at successively higher levels. The entire event can be relatively long-lived lasting for some 10 to 20 hours after the flash phase of the flare.

There are now strong observational arguments, based mainly upon Skylab data, that these flare loop systems are formed by magnetic reconnection of field lines that had been previously pulled open by the eruption of a pre-flare filament. According to the soft X-ray observations, this phenomenon is not confined only to flares but also occurs away from active regions with the eruption of quiescent prominences. Hence, we expect reconnecting loop systems to take place during periods of minimum solar activity as well as during solar maximum. If, indeed, we are seeing magnetic reconnection here then observations from space will provide a unique opportunity to study this very important phenomenon.

Strongly associated with two-ribbon flares and with eruptive prominence events without flares are coronal transients. These spectacular large-scale events (a white-light photograph of one is shown in Figure II-11) consist of magnetic loops traveling rapidly (200 to 1000 km s^{-1}) outward from the Sun into interplanetary space. They were hypothesized long ago by Thomas Gold but were first observed only recently by the

white-light coronagraphs aboard OSO-7 and Skylab. The propulsion mechanism for coronal transients is not understood. However, if the reconnection concept for two-ribbon flares discussed earlier is correct, then the coronal transient can be understood as a natural consequence of this same process. When two oppositely directed field lines reconnect, a lower loop is formed rooted to the solar surface (the flare loop). In addition, an upper loop disconnected from the surface is produced. These upper disconnected loops may provide the driving force for the transient and prominence material. A schematic illustrating how the geometrical configuration of this process might look is shown in Figure II-12. In this topology, the net upward force on the transient originates from the increasing inbalance in magnetic pressure across the structure. This imbalance is a natural consequence of the reconnection process since new magnetic flux is added beneath the erupting prominence whereas none is added above.

This, as well as other alternative theoretical concepts of the basic propulsion mechanism for transients have still not been tested by enough observations to discriminate between them. For example, a careful study of the interrelationship between flare loops as seen in soft X-rays with transients observed in white light is needed. The instrument package proposed for this mission is ideally suited to this problem. In addition, simultaneous polar and equatorial views of transients and flare loop systems will be invaluable in helping us untangle the geometrical complexities of these interesting structures.

Restructuring of the solar corona occurs on a broad range of time scales from seconds to years. The Skylab data allowed us to study changes occurring with time scales of hours to months and in some cases with changes on the order of minutes and even seconds. Unfortunately, these short time scale studies with the Skylab data were very few in number due principally to the facts that film had to be conserved in the experiments and that it was difficult to catch the rise phases of transient events such as flares. The soft X-ray experiment on the Solar Maximum Mission (SMM) spacecraft is providing excellent temporal and spectral resolution of transient events but at the cost of low spatial

resolution. What is needed for future studies is an experiment of high temporal and spatial resolution with a broad field of view, such as we propose for the SCE mission.

5. MAGNETIC FLUX: ITS EMERGENCE, MIGRATION, AND CORONAL MANIFESTATION

In previous sections we have stressed the importance of the magnetic field and its interaction with the coronal plasma in determining the large scale field regions that give rise to the solar wind. In this section, we shall be more concerned with closed field regions, and hence with flux that has more recently emerged from below the photosphere. In order of increasing size, this includes such closed loop coronal structures as bright points, emergent flux regions within active regions, active region loops, and loops of large scale connecting active regions or quiet regions of opposite polarity. Most of the Sun's soft X-ray emission comes from closed loop structures. Thus, if we are to understand the Sun as an X-ray star we must understand these closed regions.

Studies of Emerging Flux

Small closed regions of coronal emission appear in large numbers on soft X-ray filtergrams of the Sun. These features are called "bright points" and are short-lived regions of emerging magnetic flux. Past studies have established that bright points form the short lifetime end of a continuous distribution of solar activity and that during the Skylab period most of the magnetic flux on the Sun emerged in the form of bright points.

There are several remaining questions about emerging magnetic flux. Solar X-ray images obtained by rocket flights after Skylab suggest that the number of bright points on the disk is anti-correlated with traditional activity indices such as sunspot number. However, recent studies of ephemeral active regions using daily full-disk magnetograms indicate that the ephemeral regions, which can be identified with bright points, vary nearly in phase with larger active regions. This result therefore calls into question the apparent anti-correlation between bright points

and solar activity derived from the X-ray data. A three year observing period from 1987 to 1990, more than a quarter of a solar cycle, would include solar minimum and the early rise of the next solar cycle which should be adequate for observing an expected peak in the bright point numbers. The SCE Mission will, therefore, provide the data necessary for a strong test of the apparent anti-correlation between bright points and solar activity.

A less controversial but also less understood bright point phenomenon involves changes in bright point numbers over time scales of several months. Figure II-13 shows the temporal variations of high latitude ($> 30°$) and low latitude bright point populations during the Skylab period. The high latitude bright points gradually increased and then decreased during the mission. The low latitude bright points showed a different behavior. Over one longitude range covering an inactive region of the Sun there was a large increase followed by a corresponding decrease. In the other longitude range there was a sharp dip in the number of bright points which corresponded to a period of rapid growth of active regions in that longitude range. The low latitude variations suggest that a large eruptive event occurred on the Sun with a global coherence. We have no way of knowing how often such eruptions occur or how extreme they can be. A three year observing period should provide the data for exploring this phenomena, which is especially important because of its global character.

A related problem is that of active region births. In order to observe how an active region is born we need to have observations with a time resolution of less than an hour with the initial emergence of magnetic flux about two days ($\sim 30°$) east of central meridian in order to minimize the obscuration effects of other coronal features and follow the growth of the region. This again must be carried out in conjunction with good magnetic observations in order to sort out the important physical changes that lead to the development of an active region rather than the diffusion of the newly-emerged magnetic flux into the background fields.

We know that bright points occasionally produce flares in many respects similar to flares in active regions. At the present time we don't know what the light curve of a bright point flare is and we don't know why only a minority of the bright points ever flare during their brief ($\tau \sim 8$ hr) lifetimes. The combination of high spatial and temporal resolution in an X-ray telescope on the SCE can be very useful in attacking these questions.

Coronal Loops

Loops are the building blocks of coronal structure and are particularly well defined in action regions. In recent years there has been much interest in them, stimulated in part by Skylab. Their relative geometric simplicity, and the fact that solar wind losses may be neglected in their energy balance have made them attractive for theoretical study and a testing ground for physical theory. Quasi-static loop models in energy balance now seem quite well understood. The theoretical ground work for problems of static-loop stability and for dynamic loop models driven by siphon flow has been begun, but new observations are needed to test and advance this theory.

Simultaneous observations from SCE and ISPM would be of especial value. Any single view of the corona shows loops in projection. One cannot determine the heights of loops near central meridian nor the orientation of the planes of loops near the limbs. Because of their simple structures and high contrast with background features, the heights, lengths, and orientations of loops are easily determined by stereoscopic views from two spacecraft. Such views will enable us to derive the brightness distribution along the loop from which we can get temperature and pressure gradients. These observational parameters are needed in loop theories to get more accurate determinations of conductive heat losses and energy deposition functions. The latter are important since they can be related to coronal heating mechanisms.

The determination of the shape of a loop may indicate how the magnetic field differs, if at all, from a potential configuration. This would then indicate the magnitudes and directions of coronal currents. It would be necessary to have good concurrent magnetograms simultaneously with the X-ray observations in order to get the best determination of the potential fields.

6. THE CASE FOR AN ONBOARD MAGNETOGRAPH

Skylab yielded an excellent description of the static corona and showed where refinements and more data about static structures are needed; however, SCE must be equipped to study coronal evolution and dynamics. The low exposure rates of the Skylab instruments precluded detailed studies of how coronal structural and brightness changes are accomplished. Streamers, active region complexes, bright points and coronal holes were counted, described and fitted with static models, but most changes in these features took place in time scales short compared to the data rates.

Synoptic ground-based observations of photospheric magnetic fields were used quite successfully with potential field calculations to show that coronal holes coincide, more or less, with open fields. There remain many fundamental questions (e.g. why openings appear in the calculated fields up to a month before coronal holes, and why the boundaries of the observed holes do not well match the computed open field boundaries). It is unlikely that these questions will be solved by further refinements in the potential field models, using ground-based magnetic data, which vary greatly in quality from day to day. Future advances in understanding why coronal holes appear will require magnetograms that are free from varying observational conditions. Coronal hole boundaries change rapidly, faster than can be explained by the results of redistribution (diffusion) of magnetic footpoints in the photosphere. It is likely that changes in coronal holes, and changes in closed-field coronal structures as well, result primarily from magnetic instabilities triggered by subtle changes in the photospheric fields. In general, the amount of energy reaching the corona and the ability of coronal material

to escape into space is governed much more by the field than by any variation of energy flux at the photosphere. Since the magnetic flux recorded in an active region, for example, can vary by a factor of two in successive magnetograms made from the ground, it will be impossible to obtain a firm baseline for model calculations of coronal fields when an explanation for structural change is being sought. To study coronal dynamics, magnetograms should be made at least every six hours since the lifetime of the changing photospheric features, i.e., the emerging flux regions and supergranules, is of the order of a day. Note that daily magnetograms at a ground station will give inadequate time resolution, even during a run of clear, quiet days. During the Skylab mission, sustained efforts at Kitt Peak to obtain magnetograms with good time resolution were either foiled by poor weather or rendered uninteresting by a lack of simultaneous coronal activity.

On a time scale of several days, varying observing conditions, including days of no observations, will introduce errors in the lower harmonic terms of potential field expansions. These errors will hamper progress in studies of how the gross structure of the corona changes over several days and prevent adequate evaluations of solar dynamo models.

Any study of small-scale magnetic field influences on the corona will require that 2 to 3" features be followed as they move about on the surface. Only from a space platform free of varying image distortions can we hope to follow the elemental magnetic features from emergence, through several diffusion steps, to death by a subsidence, merging or annihilation. While occasional minutes of good seeing show the photospheric field distribution clearly, it has been impossible to say, for example, when a new bipolar region emerged and by how much time a corresponding coronal bright point preceded or followed the field's appearance. The persistent difficulty of simultaneously observing photospheric fields and coronal developments has kept us from knowing what the threshold is for bright point appearances. That is, at what magnetic field strength does the coronal temperature rise above about one million degrees? How long does the corona remain bright after the

underlying fields have dispersed? Do increases in active region temperature and density follow the magnetic developments closely? These questions are fundamental for understanding the solar corona.

Finally, we note reports of large variations in bright-point counts from day to day, as well as other hard-to-verify indications that magnetic flux may appear everywhere on the surface in a pattern possibly orchestrated from below the photosphere. Stable measurements of the fields everywhere on the solar disk are needed to examine this possibility. If there really are temporary global increases in bright points our approach to theories of solar magnetism would have to be profoundly changed. Global patterns of field emergence varying in a matter of days could exist and still have escaped our notice, just as large-scale pulsations did for so long.

A stable magnetograph is necessary to undertake a long-term study of solar magnetism and coronal structure. It is known that the local atmospheric conditions at ground-based observatories can change over periods of a few years. Since magnetic flux measurements are so sensitive to turbidity and scattering in the atmosphere, long term changes in observing conditions at ground-based observatories may seriously interfer with studies of solar cycle variations in the average magnetic flux or in the size distribution of magnetic features.

In principle, the requirements for higher time resolution and long term coverage can be satisfied by operating several ground-based observatories around the world. This has been attempted without success. The reason for past failures is not only the dependency on meteorological conditions; the observatories themselves could not produce consistent results. For example, in 1971, an IAU Working Group on magnetic calibration attempted to intercompare results from all the magnetographs in the world. Many important observatories were clouded out during one or more of the intercomparison intervals. The eight observatories that participated reported magnetic fluxes that varied about the mean flux by an average of 28 percent. The maximum difference between observatories was a factor of 2.2! Individual examples of unexplained contradictory

results have continued to appear in the literature. Unfortunately then, the record shows that consistent flux measurements cannot be achieved using several ground-based observatories.

7. PLASMA DIAGNOSTIC MEASUREMENTS AND THEIR INTERPRETATION

A major purpose of the SCE is to obtain quantitative information about the physical properties of the coronal plasma. Some of this information is required globally on a synoptic basis for large-scale modeling of the corona and solar wind; some is required in specific structures of smaller scale. Here we consider how this is to be obtained and some problems of interpretation.

Three-Dimensional Density Structure Above 1.5 Solar Radii

White light observations of the electron scattered corona by the White Light Coronagraph (WLC) will give the most direct information about the density and large scale structure of the corona. The technique of deriving electron density from white light photo-polarimetry was solved long ago by eclipse observers, and refined for Skylab. With observations at all position angles around the limb for half a solar rotation (14 days), the entire three-dimensional structure of the corona can be recovered by tomography. New and highly efficient numerical codes are now available for this deconvolution. The useful but restrictive assumption must of course be made that the corona changes only slowly during this 14 day period so that only the slowly varying component can be inferred. Simultaneous observations from ISPM would greatly reduce this uncertainty.

Temperature and Systematic Velocities Above 1.5 Solar Radii

About one part in 10^7 of coronal hydrogen is neutral. The chromospheric Lyman-alpha photons resonantly scattered by these few coronal hydrogen atoms is nevertheless observable, and provides a new and powerful technique for measuring coronal temperatures and velocities that will be exploited by the SCE.

In brief, the Resonance Line Coronagraph (RLC) measures the profile of this scattered Lyman-α radiation as a function of position above the Sun's limb from about 1.2 to 8 solar radii. These profiles, and similar profiles of λ1032 O VI are the basic data.

The local coronal proton temperature will be determined by measuring the profile of the resonantly scattered hydrogen Lyman-alpha line using the RLC on a synoptic basis. The shape of the observed profile depends on the thermal broadening produced by hydrogen plasma at the local hydrogen temperature and non-thermal broadening due to turbulent and solar wind velocities. To a lesser extent the profile shape depends on the position of the emitting plasma relative to the plane of the sky. In order to derive reliable temperatures from observed Lyman-alpha profiles it is necessary to measure coronal mass flow and turbulent velocities and the location of the observed region relative to the plane of the sky. All of these parameters will be determined with the proposed instrument package from measurements of (1) the coronal Lyman-alpha and O VI profiles (which give turbulent velocity information), (2) the Lyman-α, O VI and white light intensities (which give velocities--see below, and (3) synoptic data (which provide the location in three-dimensional space).

The coronal electron density is required and will be determined by measuring the polarized radiance of the visible light corona with the white light coronagraph (WLC) as described above. It is important to stress that what is desired is the local electron density, as opposed to the line-of-sight total density. To obtain the former quantity, we require a series of synoptic observations of coronal structures rotating about the limb, permitting a separation of features from background and identification of coronal regions of interest such as holes and streamers.

In regions with negligible Doppler dimming of Lyman-α (where $v \leq$ 100 km/sec) the combination of Lyman-α and white light data gives the hydrogen density n_H, electron density n_e, proton temperature ($T_p \approx T_H$) the first two of which when coupled with the ionization equation yields the electron temperature, thus enabling one to examine possible differences

between the derived proton and electron temperatures which may result from selective heating. In regions with significant Doppler dimming it is necessary to make use of the equations of continuity of mass, energy and momentum when deriving neutral hydrogen densities because the Lyman-α intensity depends on both the flow velocity and neutral hydrogen density. In this case the derivation of densities cannot be separated from modeling.

The combination of simultaneous and cospatial Lyman-α, O VI λ1032, and white light measurements provides a unique opportunity to determine the solar wind velocity as it accelerates outward from the Sun. The combined observations are sensitive to coronal flow velocities from 25 to 300 km/sec (see Fig. II-14). This sensitivity ensures that the proposed instruments are capable of measuring coronal flow velocities in the expected range. In the case of Lyman-α, the outward flow of the corona creates a Doppler shift between the rest frame of the coronal scatterer and the chromospheric Lyman-α radiation source. Fewer hydrogen atoms are capable of participating in the scattering of the chromospheric Lyman-α radiation as the solar wind velocity increases. Hence, one expects a lowering of the observed Lyman-α intensity with increased velocity or "Doppler dimming" effect.

The solar wind velocity can be determined to first order from both Lyman-α and white light measurements in the following manner: The intensity of the Lyman-α line depends upon a number of neutral hydrogen atoms along the line-of-sight which are capable of scattering the Lyman-α radiation from the chromosphere. Measurements of the intensity of the white light K-corona provide information on the number of electron along the line-of-sight. Then through the use of: (1) the temperature derived from the Lyman-α profile; (2) the hydrogen ionization equation; and (3) the electron density; the number of neutral hydrogen atoms along the line-of-sight can be determined. Since the fraction of these neutral hydrogen atoms capable of scattering chromospheric Lyman-α light depends on the solar wind velocity, a comparison of the observed Lyman-α intensity with that calculated for different solar wind velocities will yield a measurement of the solar wind velocity.

Observations of the O VI λ1032 line can be even more sensitive to the Doppler dimming effect than Lyman-α. This sensitivity arises from the fact that the transition region source of O VI radiation is much narrower than the Lyman-α counterpart and its thermal width in the corona is one-fourth that of Lyman-α (for the same temperature). The narrowness of both the source and scattering profiles make the O VI line sensitive to flow velocities below 100 km s^{-1}--a regime where the Lyman-α Doppler dimming is a relatively insensitive function of velocity.

The Doppler dimming technique is probably the only method that can be employed to determine the steady outward flow of coronal material into the solar wind and measure its variation with height in low density features like coronal holes except at the very base of the corona. Normal Doppler shift measurements are not applicable at the limb because the major velocity component of the solar wind is perpendicular to the line-of-sight. Flow velocities can be inferred indirectly from radio scintillation measurements, however, the interpretation of these observations is severely restricted by line-of-sight averages, yearly occultations of radio sources by the corona and a limited sampling of coronal regions. Although systematic outflows have been measured on the disk from Doppler shifts of EUV coronal lines, no information on the variation of the velocity with height has been obtained. Another attempt to observe the steady state material flow in the corona directly has involved the examination of Skylab WLC photographs for the presence of density inhomogeneities moving outward; no obvious motions have yet been detected. Thus, the Doppler dimming technique appears to be the only possible means of directly measuring the steady flow of the solar wind above about 1.2 solar radii.

Temperatures and Pressures from Soft X-Ray Observations

The techniques for deriving temperatures and density using the WLC and RLC in concert as described above depend on observations made above the limb and are most useful above 1.5 solar radii. Below this height soft X-ray filtergrams show the form of closed magnetic regions. In closed field regions, where the energy balance is not affected by the

loss of material to the solar wind, the heating mechanism, presumably magnetic (although a significant role for mechanical heating at least for material at "transition region" temperatures cannot be ruled out) is able to sustain material in coronal loops at temperatures ranging up to 5-10 x 10^6 K, and their material at "transition region" temperatures may well play the classical role of a medium through which the coronal material and the "chromospheric" core in a loop interchange mass and energy. Transient phenomena in active region loops may be the source of the mass and energy observed in coronal transients.

In bright points, which we presume to be compact loop structures, the maximum temperature attained is lower, and the material in the temperature range near 10^6 K may play a somewhat different role. In the open field regions ("coronal holes"), where the solar wind dominates the energy balance, material at temperatures near 10^6 K may represent the source of the mass which constitutes the solar wind flow. What role bright points play in the energy balance and dynamic behavior of coronal holes is not known. It is evident that we must determine the dynamical behavior, energy balance and structure of material covering the entire range of temperatures present in the lower atmoshpere, if we are to relate structures and processes in the lower atmosphere to structures and phenomena in the corona and in interplanetary medium. In order to be able to model the lower atmosphere, we need density, temperature and bulk velocity of coronal material over the full range of temperatures from $< 10^5$ K to 10^7 K. This in turn implies the availability of spectroheliograms at high angular and spectral resolution, in lines covering a broad range of temperatures. The soft X-ray region provides diagnostic measurements especially for the higher temperature end of this range. The high contrast in X-ray emission between coronal holes and closed field regions provides one of the best techniques for locating holes.

The soft X-ray telescope (SXT) on SCE will obtain filtergrams through a set of broad band filters. Comparing two filtergrams taken through different filters yields information on temperature and pressure for various coronal features. This technique was successfully used on Skylab and will be used again by the SCE. Another approach to

the measurement of coronal temperatures is to use a set of narrow band filters capable of isolating the emissions of individual ions, such as O VII, O VIII, Fe XVIII. Three techniques for achieving such narrow pass bands for use with the SXT are discussed in Chapter III. In order of increasing sophistications these include Ross filters, an objective crystal spectrometer, and layered synthetic microstructures.

Plasma Properties of the Base of the Corona and Transition Region

The transition region and the base of the inner corona form the lower boundary to the extended corona and solar wind. An essential task of the SCE will be to define this boundary globally on a nominal time scale of one day. By "defining the boundary" we mean determining the global distribution of a few selected parameters of important physical significance such as systematic velocity, the energy density of the non-systematic velocity field, and additional parameters derived from total line intensities. Studies of more rapidly evolving or transient structures will require the determination of these parameters at a faster rate over a limited portion of the surface. The EUV Diagnostic Spectrograph (EDS) will provide these.

The spherically symmetric models that were first used to demonstrate the existence of coronal expansion predict a very slow flow speed in the inner corona, increasing to the local sound speed between 4 to 8 solar radii, and becoming highly supersonic before reaching the Earth. But such models cannot explain the high speed wind streams and are moreover inconsistent with the expanding geometry and low density coronal holes. In sufficiently rapidly expanding geometry, the flow can be shown to reach the sonic speed very close to the Sun's surface. But theoretical modeling seems to show that thermal pressure gradients alone are not capable of accelerating the high speed solar wind even if the effects of an expanding geometry and extended heating are included. The most likely candidate for the additional accelerating force seems to be wave pressure, and considerable progress has been made in the past few years in constructing models that include both heating and pressure from alfven waves. New observations required to test and direct theory, and

to estimate the flux of mechanical energy entering the corona from below, are systematic Doppler velocities and thermal and non-thermal velocities from line widths, as a function of height in the transition region and corona. Both require EUV observations of high spectroscopic resolution.

There is now strong evidence that EUV lines formed in both the transition region and corona are blue shifted within coronal holes observed near Sun-center relative to other regions of the Sun. Figure II-15 shows an example of this effect measured in λ629 O V ($T \sim 10^5$ K). The most straightforward interpretation of this result is that the high speed flow has already begun at the level of the transition region, but it might also be a differential effect due to mass interchange. In either case it indicates that the dynamics of the atmosphere is significantly different within holes even at the very base. The EDS, thus strongly complements the RLC which provides similar data at greater heights. The EUV diagnostic spectrograph data will help derive the width, displacement and intensity of several strong emission lines (λ629 OV:λλ770,780 NeVIII:λλ609,625 MgX) arising in the transition regions and corona at all points on the Sun's disk. Scientists can: (a) Use sets of rasters as described above to derive the global distribution of persistent flows, and of the wave and thermal energy densities. (b) Study the long and short term evolution of these quantities; make more intensive and detailed studies within specific regions such as polar holes, low latitude coronal holes, active regions, quiet Sun regions and streamers lying over neutral lines. (c) Use these to provide improved models of the structure of these regions and to study basic physical processes there, make detailed studies as a function of height above the limb at the limb passage of specific regions to obtain information complementary to that obtained against the disk; study the velocity fields, structure and evolution of active phenomena such as bright points, prominences and transients; study the evolution of the transition region and inner corona underlying coronal structures; study such basic physical processes as mass exchange, departure from ionization equilibrium and diffusion at the base of the corona.

III. PROGRAM IMPLEMENTATION

1. ORBITAL CONSIDERATIONS

The aims of the mission impose these general requirements on the orbit. It should be chosen to:

(a) Assure a full 3-year life time;

(b) Be free of atmospheric extinction, i.e., have a large zenith look-out angle;

(c) Avoid the Van Allen radiation;

(d) Encounter minimum interference due to the South Atlantic Anomaly;

(e) Enable a complete set of solar observations to be made at least every six hours for synoptic purposes;

(f) Be suitable for reception of telemetry;

(g) Have the Sun in view continuously for periods as long as one hour as many times a day as practicable.

A compromise might be, for example, a circular Earth-orbit of 600 km altitude and 33° inclination, which would permit the Sun to be viewed about 65 percent of the time.

2. SCIENCE INSTRUMENTATION

As discussed earlier, the present state of both coronal and interplanetary physics makes it possible to define a number of very basic, clear, and realistic aims for the SCE and these aims in turn define the essential minimum payload shown in Table III-1 below. As discussed in Chapter II, a magnetograph is included although it was given a lower priority because, with compromise, ground-based observations could fulfill some of the mission needs.

For concreteness and for estimating spacecraft requirements, cost and need for new technology we have defined a specific suitable version of each instrument. Each of these five strawman instruments is discussed in turn below.

White Light Coronagraph (WLC)

It is necessary to have some type of instrument that is capable of determining the three-dimensional coronal densities as well as monitoring changes in coronal structures on the time scale of tens of minutes. The simplest method is to record the electron scattered coronal light or K-corona. Free electrons in a highly ionized coronal plasma scatter all wavelengths emitted from the solar surface; the brightness is directly proportional to the number of electrons and the intensity of the radiation source. Other means of determining the coronal density require the knowledge of other parameters such as the temperature and ion composition of the gas. Because the Sun's radiative output is maximum in the visible wavelength spectrum, broadband measurements are sufficient to record the necessary information in the shortest time possible. However, dust in the interplanetary medium also scatters solar radiation (called the F-corona), but fortunately its radiation close to the Sun in unpolarized whereas the scattered light from the electron gas is highly polarized. Thus, it is possible to separate the K-corona from the F-corona by obtaining coronal images through polaroid filters.

The envisioned instrument to record the K-corona structures and determine the density in the corona is an externally occulted white light Lyot coronagraph similar to those flown on Skylab and on the SMM spacecraft. Such an instrument would obtain corona images from about 1.5 to 10 solar radii from Sun center through broadband spectral filters and linear polaroids whose axes of transmission are separated by 60°. Other estimated instrumental parameters are summarized in the accompanying table. The detector for this instrument would be either a vidicon or charge-coupled device (CCD). Because of the large data rate required by the instrument even with some onboard data processing and compression, some

form of data storage must be supplied by the spacecraft (in the form of a tape recorder or bubble memory). The spacecraft, or the WLC separately, will have to be rolled around the Sun line to observe the corona at all portion angles. Parameters of a strawman WLC are given in the Table III-2.

Soft X-Ray Imaging Telescope (SXT)

A soft X-ray telescope is required to derive the form of the corona below 1.5 solar radii; to study closed field structures such as coronal loops, bright points and other evidence for recently emerged flux, and active regions; and to provide plasma temperatures and pressures, especially for the coronal material of higher temperature.

A strawman instrument is shown in Figure III-1. The details of the SXT instrument are listed in Table III-3 and compared with those of the instrument on the ISPM. It uses a single quartz grazing incidence mirror with a focal length of 152 cm, almost twice that of the ISPM instrument. Since the image size is proportional to the focal length, and the same charge coupled device (CCD) is used as the detector, the spatial resolution of the strawman SCE instrument is better than that of the ISPM instrument by a factor of 2. The CCD requires a passive cooling scheme and operates in a "dithering" mode which improves the spatial resolution in one dimension by a factor of 3 by essentially taking three images each displaced by one third of a pixel from each other. Also, only one quadrant of the Sun can be viewed at any time with the CCD, so four pointings are needed to obtain a full image. A data processor buffer is required, since a large number of bits are read out in a short time for each image, and these must be "smoothed out" for a uniform telemetry rate.

The basic telescope uses broadband filters similar to those used on SMM. As discussed in Chapter II, spectroheliograms in the light of individual lines, or in the light of line multiplets which have common dependence of their excitation function on temperature can provide improved diagnostics. Described below are three techniques which can accomplish this objective with varying degrees of completeness and precision, and which involve different degrees of development. These three techniques are in order of complexity and also of technical feasibility:

(a) The use of Ross Filter Spectroscopy to isolate line multiplets,

(b) The use of Objective Crystal Spectrometer to generate high and medium wavelength resolution spectroheliograms, and

(c) The use of optical surfaces coated with layered synthetic microstructures (LSM), which will produce moderate wavelength resolution spectroheliograms at very high angular resolution.

The properties of these three approaches are shown in Table III-4 along with the properties of the basic soft X-ray filtergraph. In Table III-5 the impact of each instrument on the overall instrument parameters is given. In all cases, no additional detector is required, since the same detector used for soft X-ray filtergrams will be used for X-ray and XUV spectroheliograms, and the envelope of the soft X-ray telescope is not greatly modified by the addition of the capability for high resolution, soft X-ray and XUV spectroheliograms. Each of the configurations proposed is discussed briefly below.

The Ross Filter Spectrometer makes use of the property of thin X-ray filters so that the transmission of two filters of the proper thickness, composed of adjacent elements in the periodic table, is very nearly the same except between the K or L edges of the elements. If X-ray images taken with such filters are subtracted, the subtracted image represents the flux between the two K or L edges. Using appropriate filter pairs, the regions of lines of O VIII, Fe XVII, O VII, and others may be isolated. As discussed in Chapter II, using a set of 8 to 10 Ross Filter pairs, lines covering the temperature range from 1.5 to 12 x 10^6 K may be observed, with a modest increase in complexity in the basic soft X-ray filtergraph configuration.

The principal of the Objective Crystal Spectrometer is illustrated in Figure III-2. The Objective spectrometer selects a strip of the solar disk, which is then imaged in the wavelength λ_o, which satisfies the Bragg condition. Adjacent strips of the Sun are imaged at wavelenth $\lambda_o \pm \delta\lambda$, where $\delta\lambda = 2d \cos\theta \sin\alpha$, where α is the angular displacement of the strip from the central strip. For each strip, the wavelengths accepted

are a convolution of the crystal rocking curve and line profile. The spectrum and the disk are scanned by scanning the double crystals, maintaining the (1, -1) orientation. If the inherent rocking curve of the crystal is narrow, both line profile and photometric observations are possible. Note that this configuration is not afflicted with the problem of overlapping images in different lines which causes confusion in the interpretation of objective grating observations. For each line in which an image is desired, an individual crystal array is required. At short wavelengths (3 to 25A) natural crystals with excellent properties are available. At longer wavelengths, artificial crystals (or LSM's) are available with wavelength coverage up to several hundred angstroms. At longer wavelengths, the spectral resolving power which can be achieved is modest.

Recently Barbee and Keith have shown that it is possible to construct multilayered structures, consisting of alternate layers of dissimilar elements laid down by evaporation, which have excellent properties as Bragg Diffractors. These structures are called layered synthetic microstructures (LMS's) by Barbee and Keith, and can be made with 2d spacings from ∿25A to >400A, with as many as several hundred layers. They can be placed on any smooth surface, such as highly polished glass. It seems probable (although it has not yet been demonstrated) that normal incidence mirrors for X-ray and XUV wavelengths can be fabricated using the LSM technique. These mirrors would also have the property of wavelength selection with $\lambda/\Delta\lambda$ as high as 500-1000 at certain wavelengths. A research proposal to develop such mirrors by Stanford, Jet Propulsion Laboratory and Lockheed is currently under review at NASA. In Figure III-2c an optical configuration, using a set of such mirrors placed on a wheel is shown in cross section. Note that such a configuration can achieve magnification as well as wavelength selectivity, allowing an improvement in angular resolution, which is determined by the plate scale and the pixel size of the CCD selected.

Resonance Line Coronagraph (RLC)

The Resonance Line Coronagraph used together with the White Light Coronagraph provide a powerful tool for probing the three-dimensional temperature, density and velocity structure of the corona in the critical

region where the solar wind is accelerated. The process by which these quantities are derived from the observations are considered in Chapter II. Briefly, the RLC measures the profile of the Lyman-alpha line (λ1216 HI) as a function of height and position angle above the Sun's limb. The profile of this line provides information about the velocity distribution of hydrogen atoms along the line of sight, and hence information on the coronal temperatures. The white light measurements provide information about the electron density along the line of sight, which when coupled with the temperature information provided by the profile measurements can be used to determine the neutral hydrogen density. Since the intensity of the Lyman-α line depends on the neutral hydrogen density and the outflow velocity of the solar wind, the combination of white light and Lyman-α intensity measurements provide information on outflow velocities for flows with velocities greater than about 100 km per second. Other spectral lines such as O VI λ1032, which have a different sensitivity to outflow velocities, can be used to probe lower speed outflows, and to separate thermal and non-thermal velocities. The overall objective of the pair of coronagraphs is to obtain information on the three-dimensional temperature, density, and velocity structure of the corona above 1.5 solar radii and monitor its evolution with time.

The RLC consists of a 1.5 meter grating spectrograph with photoelectric detection system, and off-axis parabolic primary mirror (0.8 meter focal length) and an occulting system which employs a rectangular entrance aperture and internal straight edge occulter. The primary mirror is rotated in the direction of dispersion to scan from 1.2 to 8 solar radii. The spectrograph will be stigmatic and employ a two-dimensional array detector at Ly-α (and perhaps additional arrays at other wavelengths such as O VI λ1032) measuring the line profile (approximately 0.1 Å resolution) in the direction of dispersion and providing spatial resolution perpendicular to the direction of dispersion. The dimensions of the instrument are about 3 meters by 0.8 meters by 0.6 meters. The approximate mass will be 200 kg, power 100 watts, and telemetry rate 2 to 4 x 10^5 bps. Because a linear occulting system is employed, the field of view of the instrument will be about 45 arc min by 100 arc min with the long dimension in the radial direction. In order to sample other coronal segments the instrument or spacecraft must be rolled. Typical times for

acquiring data at a given position of the slit (which is tangent to the limb) are several seconds at r = 1.5 solar radii and one minute at r = 4.0 solar radii in a quiet region. The mirror scanning system is programmable in order to permit tradeoffs between the size of the spatial field covered, number of radial positions within that field that are sampled, and time devoted to each position. This is needed in order to allow for both long duration observations in coronal holes where the intensities are low, and short duration observations with good time resolution for studying transient phenomena. A summary of instrument parameters is given in Table III-6.

EUV Diagnostic Spectrometer (EDS)

The EUV Diagnostic Spectrometer is required for measuring the velocity field and other plasma properties in the transition region and at the base of the corona at all places on the disk and immediately above the limb. These global measurements are essential to provide the lower boundary for modeling the corona and solar wind.

A basic observational parameter needed to constrain theory and to infer the deposition rates of energy and momentum, is the systematic velocity field as a function of height from the transition region up through the inner corona. As described above the Resonance Line Coronagraph, in combination with the White Light Coronagraph, can provide information on outflow velocities in excess of 100 km/sec at heights above 1.5 solar radii at the Sun's limb. The EUV Diagnostic Spectrometer described here will provide complimentary information about systematic flows of 1 km/sec or more in the transition region and in the base of the inner corona, as well as plasma temperature and pressures from line widths and intensities for $T \lesssim 1.5 \times 10^6$ K. The diagnostic techniques of the EDS are discussed in Chapter II.

The strawman EUV Diagnostic Spectrometer (Figure III-3) consists of an off-axis parabolic telescope of 0.3m focal length and 7 cm^2 aperture that feeds an f/10 slit spectrograph. The spatial resolution is 20 arc sec. The spectrograph is a single element Rowland mount employing a 7200 groove/mm concave grating of 1.2m radius of curvature, providing a linear

dispersion of 1.14/mm in first order. In the high resolution mode the spectrum from 608A to 638A, or alternatively from 760A to 790A is formed on a 1 x 1024 multichannel detector with a resolution of 0.028A to obtain a spectrum in 0.4 seconds. The detector consists of a microchannel plate and CODACON readout scheme. In the low resolution mode, the spectrum from 400A to 1000A is scanned past a channel electron multiplier (CEM) detector by rotating the grating to provide 1A resolution. Offset pointing and rastering over ± 20 arc min is affected by rocking the telescope objective mirror. An onboard absolute wavelength standard makes it possible to derive absolute velocities. The instrumental parameters of the EDS are summarized in Table III-7.

In this example, the two wavelength regions were chosen for high resolution studies because they contain resonance lines of O V, Ne VIII and Mg X, whose heights of formation span the middle transition region to the base of the inner corona. The grating probably cannot be optimized for more than two such regions, but nearby regions can be used with some loss in resolution.

Magnetograph (MAG)

The coronal magnetic field is a major element in coronal and solar wind physics that cannot be measured directly, but can only be inferred from the continuation of photospheric fields. Measurements of the longitudinal component of the photospheric field at all points on the visible disk, nominally on a daily basis are essential to the aims of the mission. As discussed Chapter II, these can best be obtained from a magnetograph on SCE even though, with some compromise, ground-based observations could fulfill the most crucial needs of the missions.

Magnetographs were designed and proposed for the ISPM but not flown on it. Based on these designs, parameters of a strawman magnetograph for SCE are given in Table III-8.

3. SPACECRAFT REQUIREMENTS AND NEW TECHNOLOGY

The scientific instrument parameters bearing most directly on spacecraft requirements are summarized in Table III-9. The spacecraft, or a section of it, must be able to locate Sun-center and offset-point from it with an accuracy of ± 10 arc sec. The WLC and the RLC require that the spacecraft have the ability to roll to any position angle about the spacecraft-Sun line, or; that the WLC and RLC, copackaged, rotate with respect to the spacecraft. If this roll were to be provided only by the slow precession of the spacecraft it would severely limit their ability to study large scale coronal structure and velocity. All of the instruments are designed to operate with the spacecraft pointed at Sun-center except for the SXT, which requires a 2 x 2 spacecraft raster to observe the entire disk. This is in conflict with the other instruments, but since whole-disk SXT observations on a synoptic basis are essential, this seems unavoidable except by severely compromising SXT resolution. The magnetograph appears to have a relatively small impact on spacecraft and mission requirements.

Most of the instruments in the strawman scientific payload are similar to instruments that have already been flown or are now being developed for flight. The WLC is similar to instruments flown on Skylab and SMM. A package containing a WLC and RLC have been flown on two successful rocket flights by the Center for Astrophysics and the High Altitude Observatory and is being developed for a Spacelab flight, but observations thus far have been obtained only in λ1216 H I. Coronagraphic observations at λ1030 O VI have not yet been attempted.

The strawman SXT was prepared by American Science and Engineering based on their experience on Skylab and on their development of an X-ray telescope for ISPM employing a CCD detector. The auxillary optics suggested for the SXT beyond the use of filters is based on a study at Stanford by A.B.C. Walker and, as discussed in the previous section, would require some new development. The strawman EDS uses a design by G. Rottman at the Laboratory for Atmospheric and Space Physics, and successfully carried on two rocket flights (although the existing rocket instrument does not have the ability to scan the grating or rock the objective mirror).

A suitable magnetograph has never been flown on a spacecraft. The strawman MAG parameters were provided by D. Rust of American Science and Engineering. They are an extrapolation from a design studied at American Science and Engineering for the ISPM. This would be new development.

We note finally that the large data rates and accumulations call for new developments in onboard data compression, storage and even analysis. But these will have to be addressed by NASA in other contexts if the new detector arrays are to be exploited, and for other planned missions.

Table III-1

SCE Strawman Payload

White Light Coronagraph	(WLC)
Soft X-Ray Telescope	(SXT)
Resonance Line Coronagraph	(RLC)
EUV Diagnostic Spectrometer	(EDS)
Magnetometer	(MAG)

Table III-2

White Light Coronagraph (WLC) Parameters

Dimensions	
Length	3.0 m
Width	0.3 m
Height	0.3 m
Mass	80 to 90 Kgm
Power	50 watts*
Pointing	±10 arc sec from Sun center ±2 arc sec per 5 min of jitter
Resolution	10 arc sec
Field of View	1.5 to 6 R_o for 10 arc sec resolution 1.5 to 10 R_o for 20 arc sec resolution
Exposure Times	∿1 min/image
Image Size	1000 x 1000 pixels
Data Rates	Standard: 8 images/orbit Special Events: 14 images/day Average: 150 images/day
Without Data Compression	8 bits/pixel; 8×10^6 bits/image 1.2×10^9 bits/day; (14 Kbps average)
With Data Compression	2 bits/pixel; 2×10^6 bits/image 3×10^8 bits/day; (3.5 Kbps average)

*Average power without active thermal control system

Table III-3

Soft X-Ray Telescope (SXT) Parameters for SCE

Compared with those for ISPM

	SCE	ISPM
Focal Length	152 cm	83 cm
Mirror Diameter	17.8 cm	14 cm
Size of Solar Disk in Focal Plane	1.41 cm	0.77 cm (at 1 A.U.)
Mirror Collecting Area	30 cm^2	15 cm^2
Angular Field per Pixel (with dithering)	1.3 arc sec x 4 arc sec	2.5 arc sec x 7 arc sec
Mirror	Quartz	Beryllium
Detector	256 x 320 RCA CCD	256 x 320 RCA CCD
Mass	45 kg	
Power	32 watts	
Detector FOV	17 arcmin x 21.4 arcmin (2 x 2 matrix required for full disk)	31 arc min x 39 arc min
Detector Cooling	Passive	
Optical Bench	Aluminum	
Number of Bits in One Sequence of Images with One Filter	12 x 256_6 x 320 x 4 = 4 x 10^6 bit (4 exposures plus dithering)	
Maximum Telemetry Rate Assuming One Sequence per Minute	66 kbps	
Minimum Telemetry Rate Assuming One Sequence per Seven Minutes (One Solar Image per Orbit in each of two filters)	10 kbps	

Table III-4

Technique	$\lambda/\Delta\lambda$	Wavelength Range	Angular Resolution	Development Period
Filtergraph	2-3	3-600Å	1.3"x4"	No development needed
Ross Filter	10-12	3-30Å	1.3"x4"	No development needed
Obj. Spect.	500-10,000	3-1000Å	1.3"x4"	Modest development
LSM Optics	500-1,000	75-1000Å	0.4"x1.3"	Considerable developmen

Table III-5

Envelope for Various Soft X-Ray/XUV Spectroheliograph Configurations

Configuration	Length	Cross Section	Weight	Power
Basic Filtergraph	185 cm	25x25 cm	45 kg	30 watts
Ross Filtergraph	185 cm	25x25 cm	45 kg	30 watts
Objective Spectrograph	210 cm	35x35 cm	52 kg	32 watts
LSM Optical Conf.	185 cm	25x25 cm	48 kg	31 watts

Table III-6

Resonance Line Coronagraph (RLC) Parameters

Dimensions	
Length	3.0 m
Width	0.8 m
Height	0.6 m
Mass	200 kg
Power	100 watts
Resolution	1.0 arc min
Field of View	45x100 arc min
Scanning	1.2 to 8.0 solar radii
Telemetry Rate	200 to 400 kbps

Instrument or Spacecraft must be rolled

Table III-7

EUV Diagnostic Spectrometer (EDS) Parameters

Dimensions	
Length	1.5 m
Width	0.3 m
Height	0.3 m
Mass	50 kg
Power	15 watts*
Resolution	20 arc sec
Field of View and Pointing	±20 arc min provided by rocking telescope objective
Spectrum	
High resolution mode	1024x1 elements in 0.4 sec in ranges λλ608-638Å or λλ770-790Å; resolution: 0.028A
Low resolution mode	λλ400-1400Å; resolution: 1A
Maximum data rate	41 Kbps

*Orbit average without active thermal control

Table III-8

Magnetograph (MAG) Parameters

Dimensions	
Length	1.0 m
Width	0.2 m
Height	0.2 m
Mass	20 kg
Power	15 watts
Pointing	disk center ±2 arc min
Field of View	35 arc min
Resolution	2.5 arc sec
Quantities Measured	Photospheric longitudinal magnetic field and velocity in 4 spectral lines
Precision	1 gauss
Range	1-2000 gauss
Duty cycle	Full disk once per hour
Data	1.5×10^6 measurements per hour or 5×10^3 bits per sec.

Table III-9

Spacecraft Requirements of the Strawman

Scientific Instrument Package

Instrument	WLC	SXT	RLC	EDS	MAG	Total
Mass (kg)	85	45	200	50	20	400
Volume (m^3)	0.27	0.23	1.44	0.14	0.04	2.12
Largest dimension (m)	3.0	2.1	3.0	1.5	1.0	----
Power* (watts)	50*	32	100	15*	15	212
Maximum data rate (Kbps)	130	66	400	41	5	----
Requires sun center pointing?	yes	no	yes	no	no	----
Can operate with Sun-center pointing?	yes	yes	yes	yes	yes	----
Requires s/c raster or offset pointing?	no	yes	no	no	no	----
Requires s/c or instrument roll?	yes	no	yes	no	no	----

General pointing requirements: Absolute pointing accuracy with respect to Sun center ± 10 arcsec.

Pointing stability with 5 minutes of jitter: ±2 arcsec.

*Does not include power required by active thermal control.

FIGURE CAPTIONS

I-1: Recommended Time Line for the Solar Corona Mission and Related Missions.

II-1: Caption on Figure

II-2: 27-day per line Bartels display of interplanetary magnetic field (IMF) polarity, coronal hole occurrence data (plus 3 days to allow for Sun-Earth transit time), solar wind speed, and geomagnetic disturbance index C9 (left to right); 27-day average sunspot number R is in the narrow strip at the far right. Each line of picture elemetns represents one 27-day rotation period of the Sun. Thus picture elements vertically above or below one another represent phenomena associated with a single longitude on the Sun. Holes were considered only if they occurred within 40° of the solar equator. Prior to 1974 the hole observations were obtained from X-ray and XUV images by OSO-7 and Skylab, and thereafter they were obtained from ground-based helium images.

IMF	HOLES	WIND	C9	R
+: red	+: red*	300km/sec: dark blue	0: very dark blue	:0
-: green	-: green*		1: dark blue	:1-15
other: blue	none: blue	400: light blue	2: light blue	:16-30
		500: orange	3: purple	:31-45
		600: dark yellow	4: dark orange	:46-60
*Weak holes have been		700: light yellow	5: light orange	:61-80
assigned darker shades		800: white	6: dark yellow	:81-100
or color.		no obs yet: black	7: light yellow	:101-130
+: North polarity field lines toward Sun			8: white	:131-170
-: South polarity field lines away from Sun			9: white	:171-

II-3: Soft X-ray observations of coronal holes during 1973-1978 (courtesy of AS&E).

II-4: A sequence of white-light coronal images (2.6-8.0R_o) during three consecutive limb passages of a large, southern-hemisphere coronal hole (courtesy NRL). The hole is visible alternately in the SE, SW, and SE quadrants as a streamer-free region ranging from approximately 65° latitude on one side of the south pole to a position near the equator on the other side.

II-5: Panel (a) is a detailed neutral line map for 19 October 1973 prepared by P. McIntosh and coworkers. Panels (b) through (d) show the X-ray solar corona during the birth of a coronal hole indicated by the arrow at the left. The arrow in the lower right points to a coronal depletion associated with a bright but fading coronal transient. From Solodyna et al (1977).

II-6: An Fe XV (λ285 Å) coronal spectroheliogram from Skylab with a photospheric magnetogram of the same field. One can easily see that magnetic field lines extend a great distance through the corona to interconnect bipolar magnetic regions.

II-7: Sketches illustrating one interpretation of the spectroheliogram-magnetogram observations. a) Old field prior to eruption of a new bipolar magnetic region (BMR). b) Old field and incipient BMR. c) Old field interacting with new BMR. d) The reconnected fields.

II-8: Tomographic views obtained of a target region T on the Sun. An image with n x n elements is obtained from the ISPM spacecraft at a high latitude position. In the coordinate system corotating with the Sun the SCE spacecraft will appear to rotate 13° eastward per day. The X-ray telescope on the SCE spacecraft can also take images of n x n elements at daily intervals to be used with the ISPM image for tomographic reconstruction of the region T.

II-9: Fieldline and streamline configuration corresponding to an exact solution of the solar wind and magnetohydrodynamic equations. This topology is intended to approximate the solar corona during solar minimum and represents a simple dipole whose magnetic fieldlines have been pulled outward by the solar wind.

II-10: An exact MHD solution of a coronal streamer-coronal hole model. The model has holes in the polar regions and a single streamer encircling the equator.

II-11: White-light photograph of a coronal transient obtained with the High Altitude Observatory white-light coronagraph experiment onboard Skylab. The black circle is not the Sun but the occulting disc of the instrument used to block out photospheric light. The size of its image is 2 solar radii. This particular transient traveled outward from the Sun at about 500 km s^{-1}.

II-12: Schematic of a possible two-ribbon flare configuration with an accompanying coronal transient. The neutral line in the figure is the point where magnetic field merging and reconnection occurs forming the flare loops below and transient above. The neutral line rises slowly (a few km s^{-1}) whereas the transient moves upward with a much higher speed.

II-13: The average number of X-ray bright points per observation, per 60° longitude interval during 1973. The upper curves show the numbers of bright points at low latitudes divided into two bins, and the lower curve shows the high latitude points for north and south combined. From Golub and Vaiana (1980).

II-14: The normalized intensity of Ly-α and O VI λ1032 as a function of flow velocity.

II-15: Systematic velocity in the transition region measured along a line on the Sun's disk crossing a well defined low latitude coronal hole (CH). Note the apparent outflow. The region to the left of the hole is a quiet unipolar region. (courtesy J. Rottman, LASP).

III-1: A possible Soft X-ray Telescope configuration.

III-2a, b, c: Caption on Figures

III-3: Caption on Figure

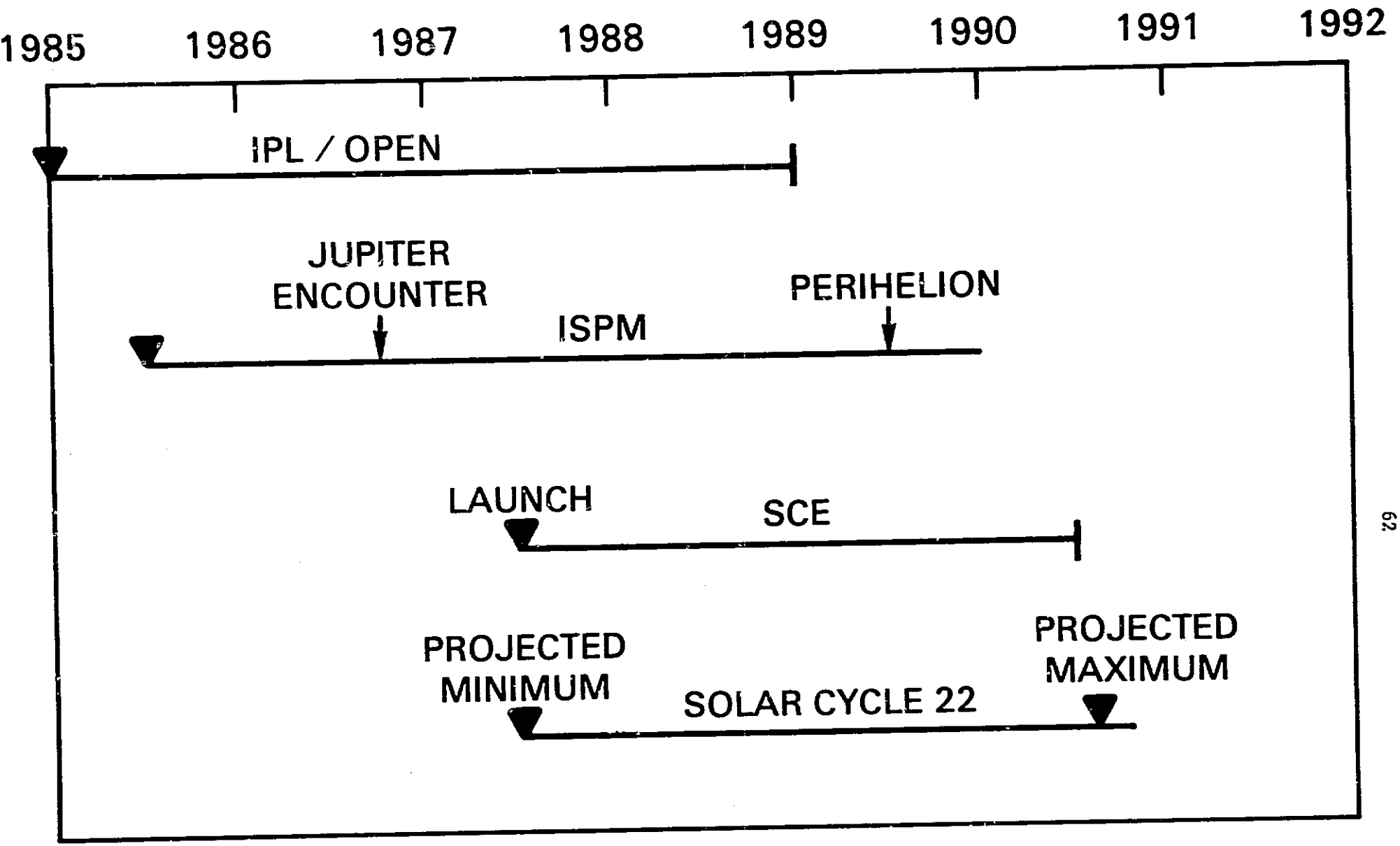
1985
1986
1987
1988
1989
1990
1991
1992
IPL / OPEN
JUPITER
ENCOUNTER
ISPM
PERIHELION
LAUNCH
SCE
PROJECTED
MINIMUM
SOLAR CYCLE 22
PROJECTED
MAXIMUM

FIGURE I-1

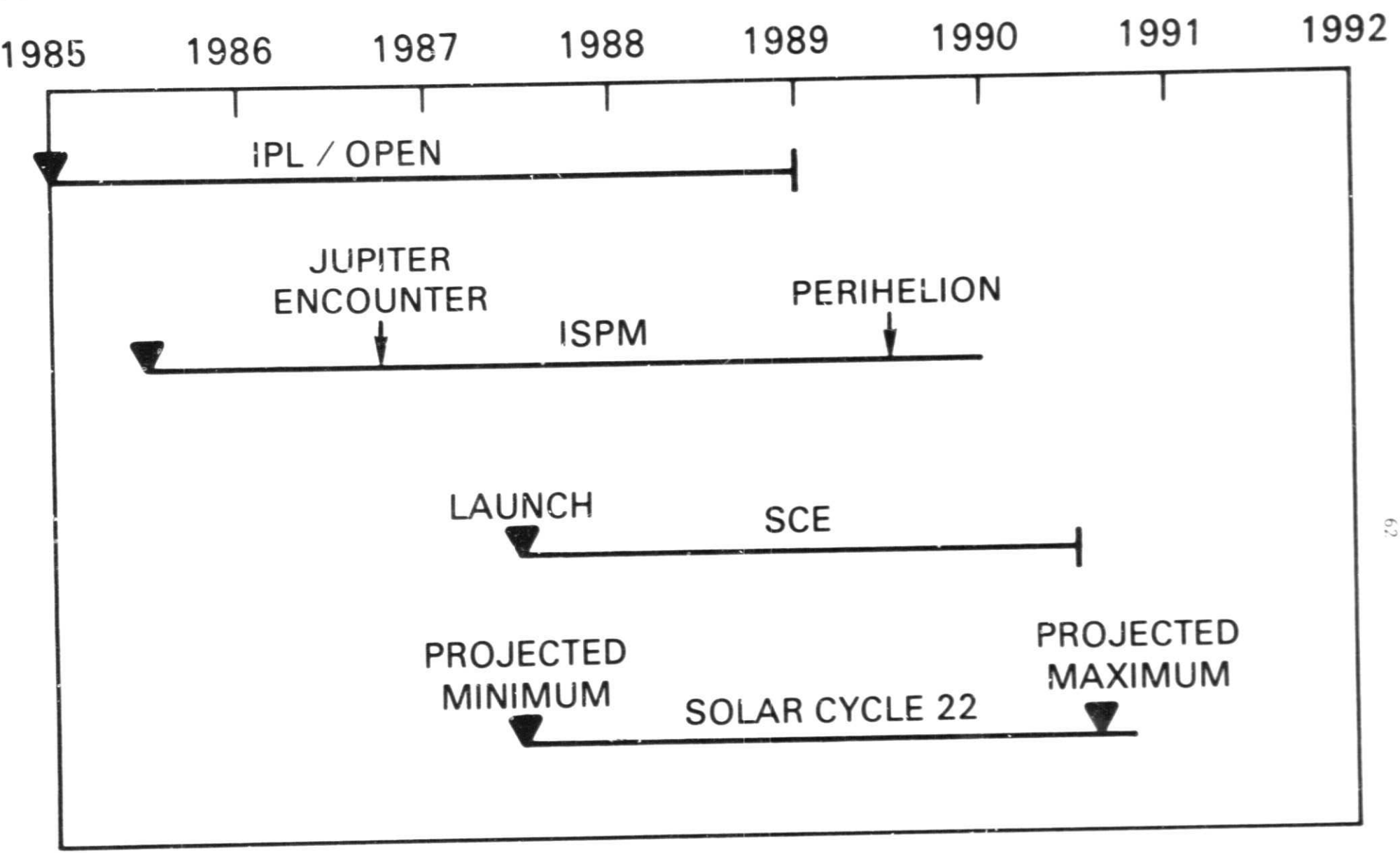
1985
1986
1987
1988
1989
1990
1991
1992
IPL / OPEN
JUPITER
ENCOUNTER
ISPM
PERIHELION
LAUNCH
SCE
PROJECTED
MINIMUM
SOLAR CYCLE 22
PROJECTED
MAXIMUM

FIGURE I-1

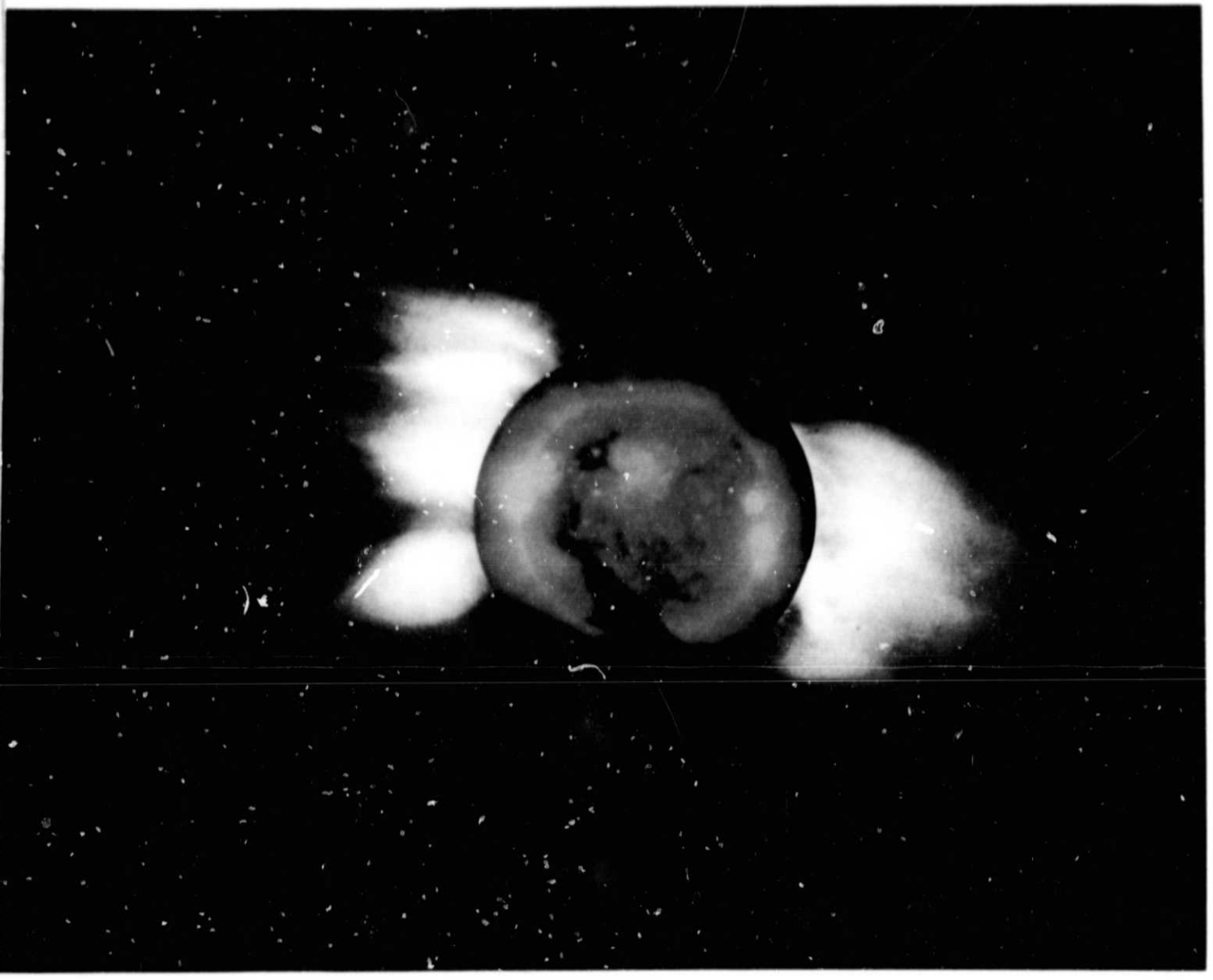

30 JUNE 1973 TOTAL ECLIPSE OF THE SUN

Outer Corona in White Light
1250 UT; from Loiyengalani, Kenya, Africa

HIGH ALTITUDE OBSERVATORY
NATIONAL CENTER FOR ATMOSPHERIC RESEARCH
BOULDER, COLORADO

Inner Corona in Soft X rays
1145 UT; from Skylab ATM

SOLAR PHYSICS GROUP
AMERICAN SCIENCE AND ENGINEERING
CAMBRIDGE, MASSACHUSETTS

FIGURE II-1

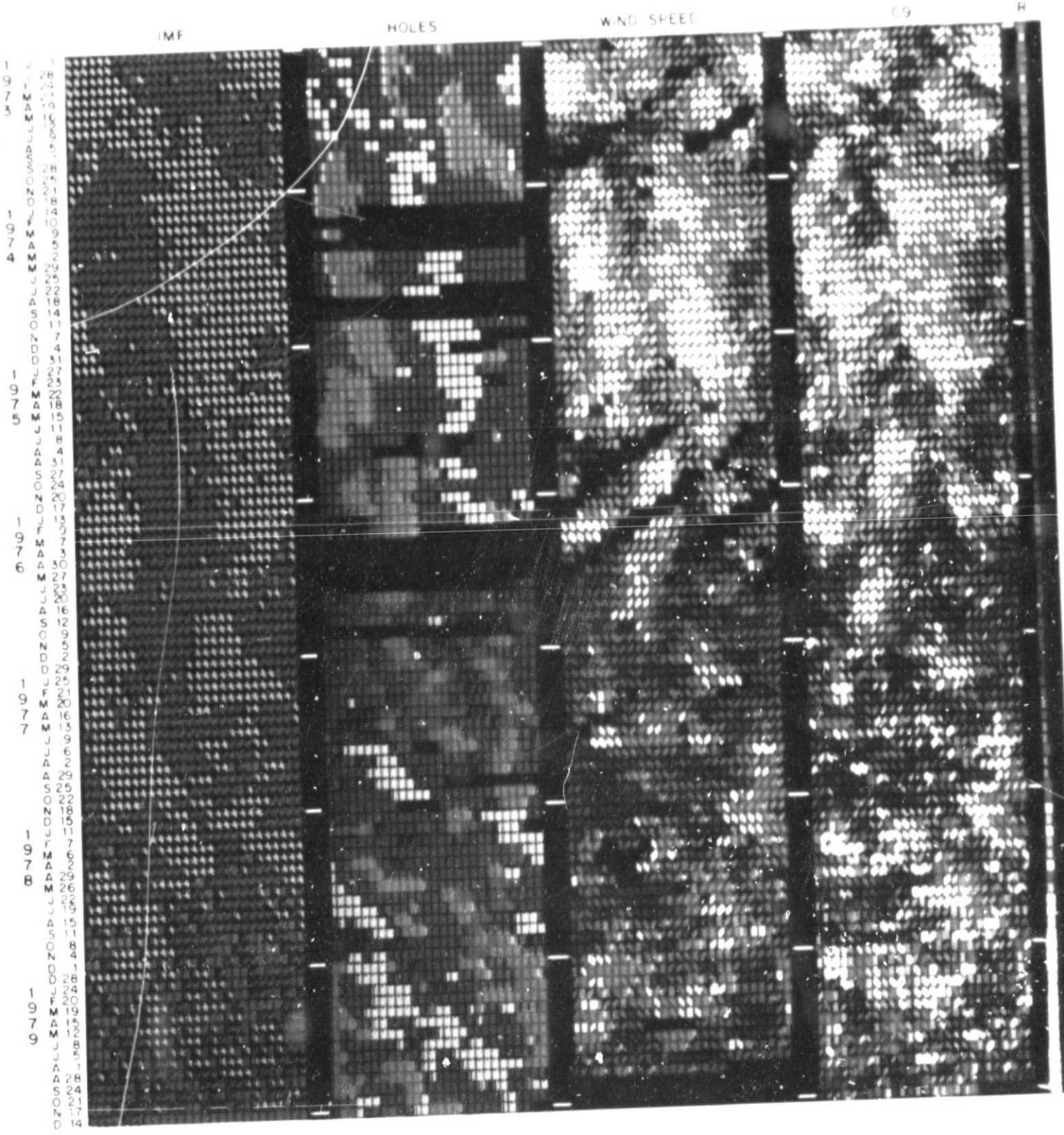

FIGURE 11-2

CORONAL X-RAY OBSERVATIONS
1973 - 1978

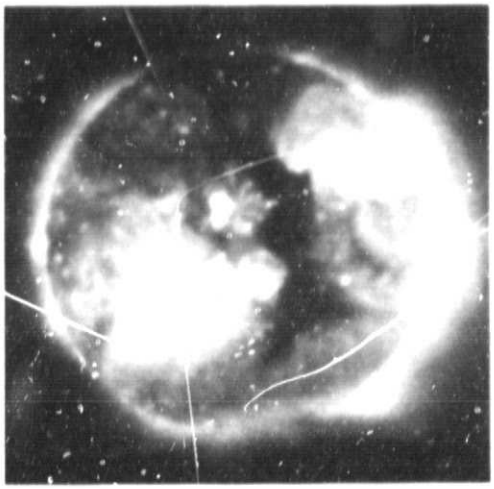

1 JUNE 1973

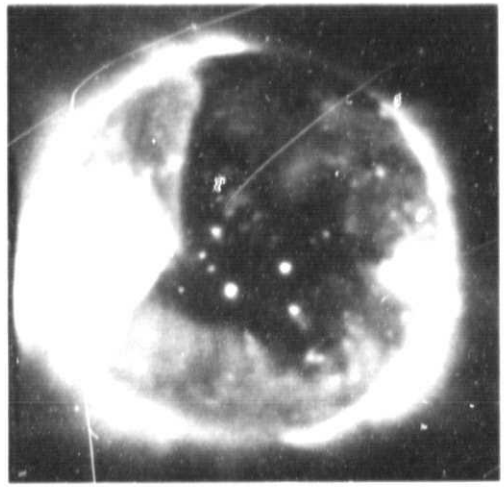

27 JUNE 1974

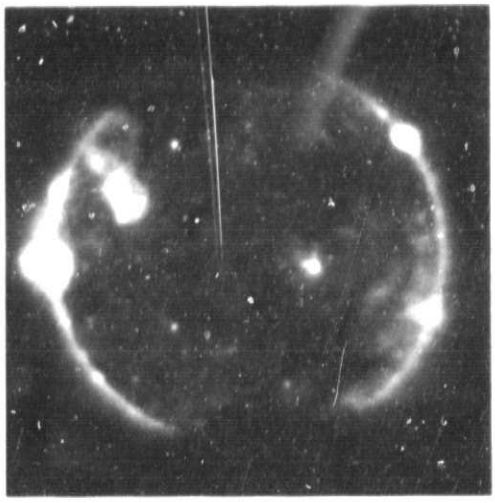

17 NOVEMBER 1976

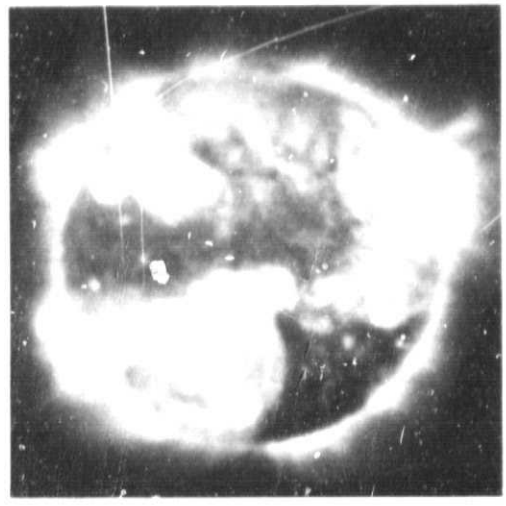

31 JANUARY 1978

FIGURE II-3

FIGURE II-4

FIGURE II-5

FIGURE II-6

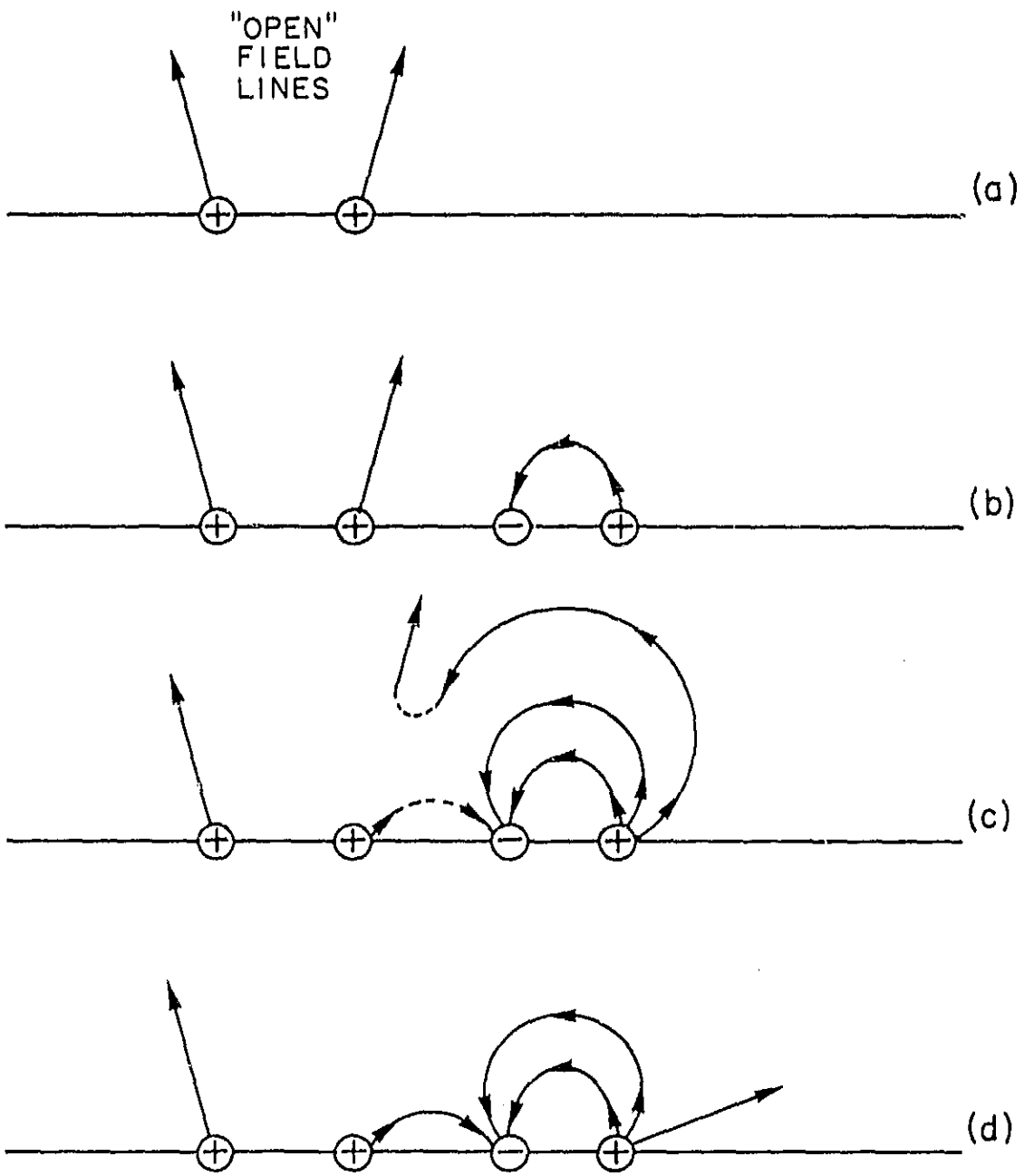

Sketches illustrating our interpretation of the spectro-heliogram-magnetogram observations. (a) Old field prior to eruption of new BMR. (b) Old field and incipient BMR. (c) Old field interacting with new BMR. (d) The reconnected fields.

FIGURE II-7

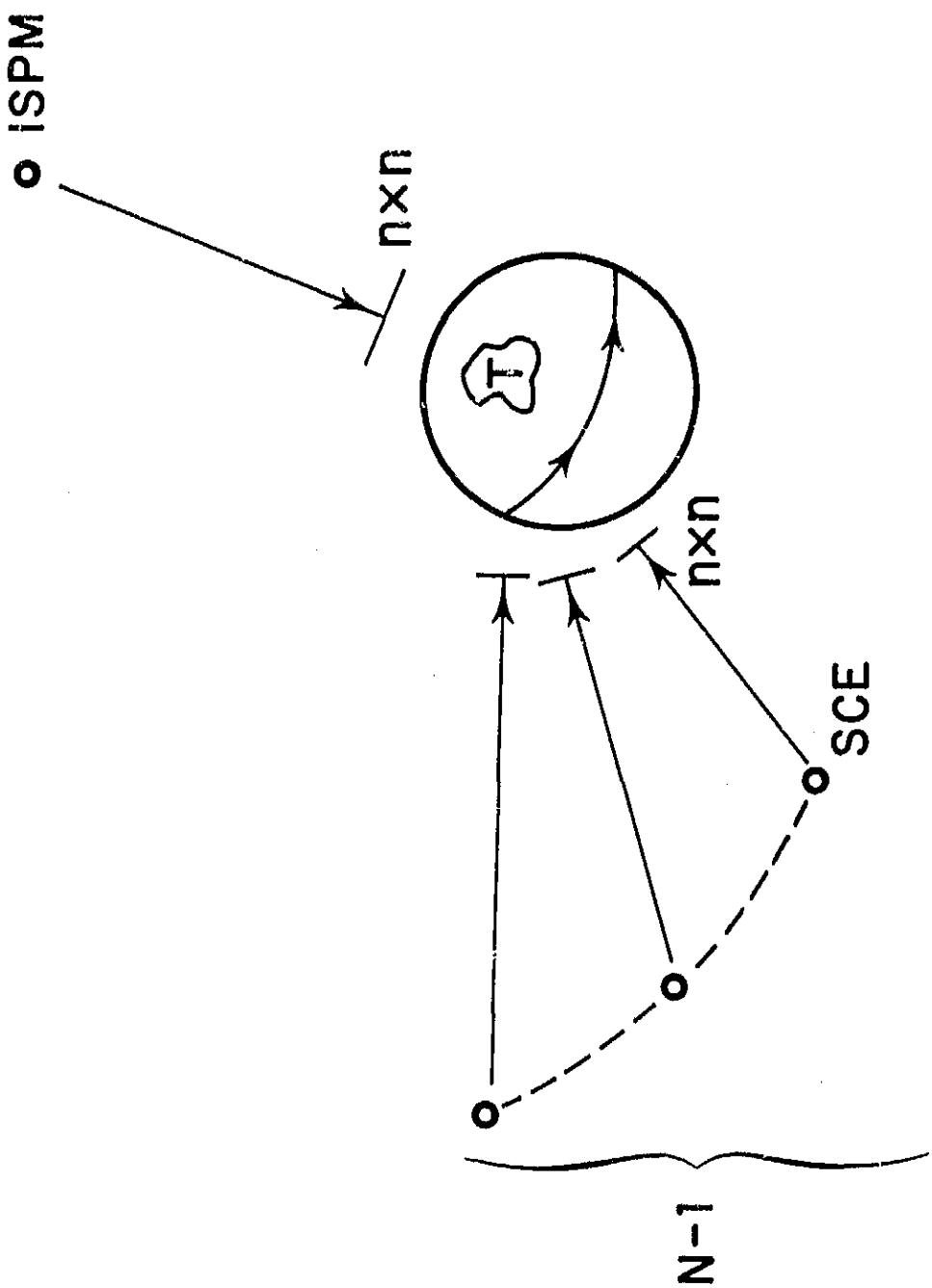

FIGURE II-8

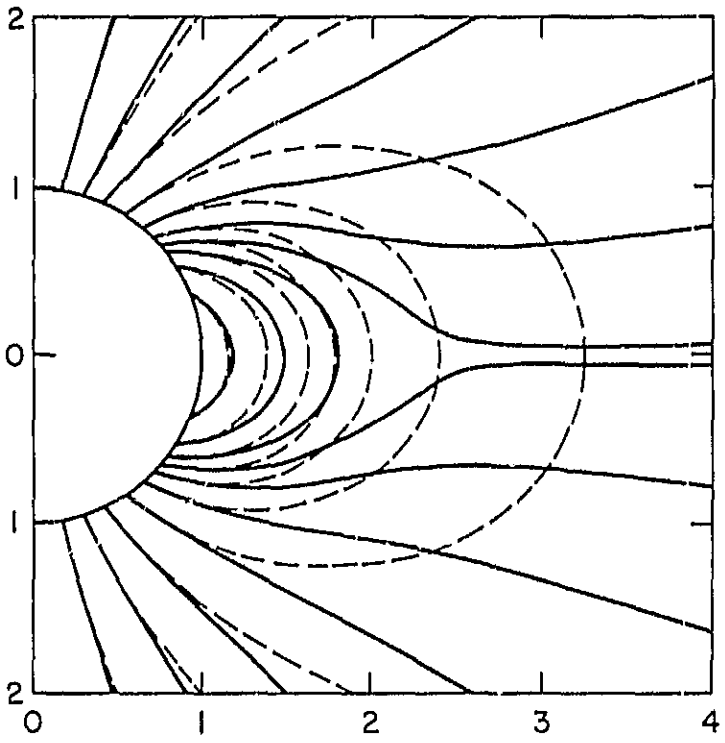

The magnetic field geometry computed by Pneuman and Kopp (1971) for equilibrium of an isothermal corona with a dipole magnetic field imposed on the base of the corona. Expansion into interplanetary space occurs along the open magnetic field lines from the "polar" regions. The dashed lines indicate a pure dipole geometry.

FIGURE II-9

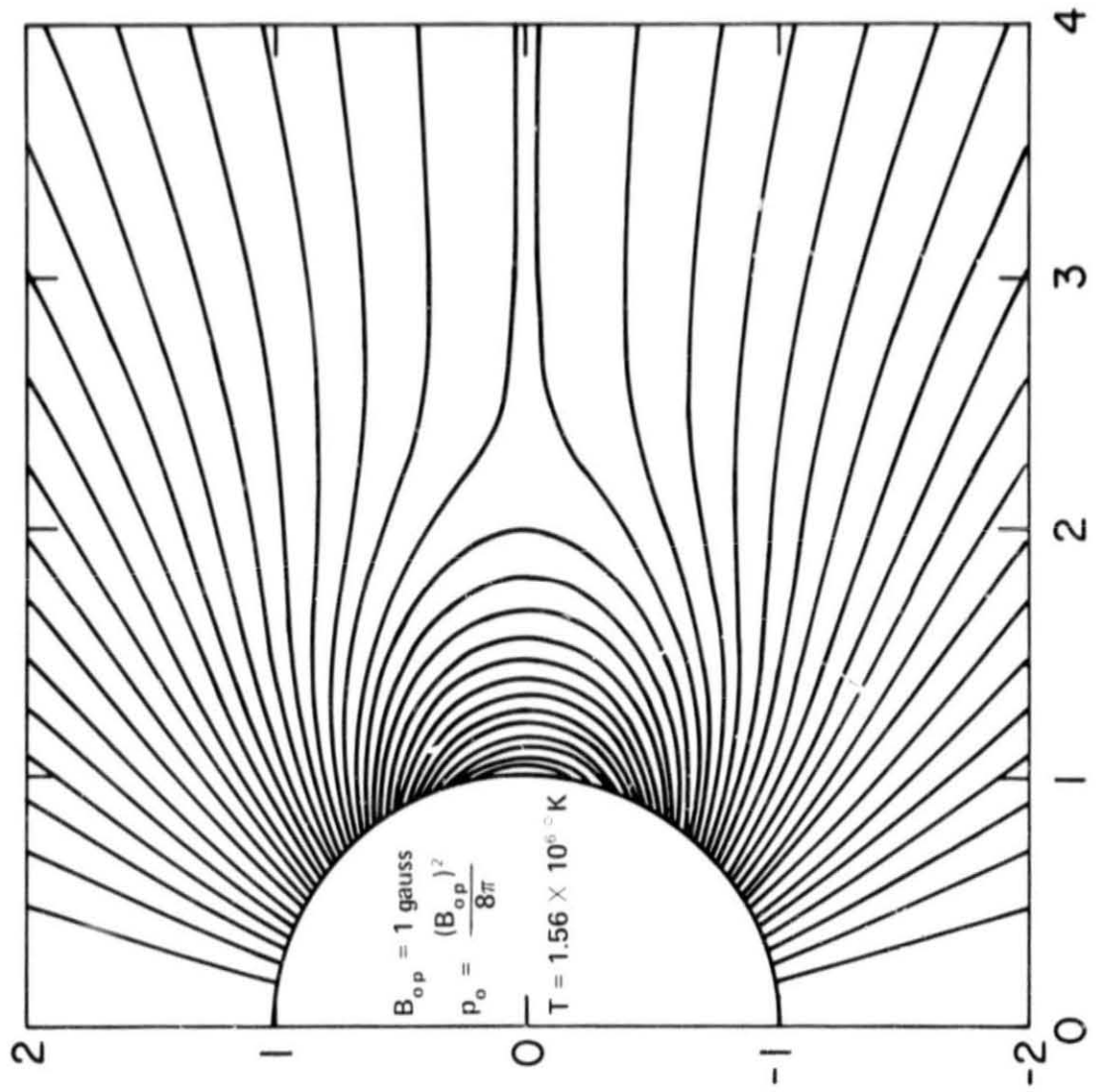

FIGURE II-10

10 June 1973
09h43m GMT
9 Second Exposure, Unpolarized

ATM SKYLAB WHITE LIGHT CORONAGRAPH EXPERIMENT
HIGH ALTITUDE OBSERVATORY
NATIONAL CENTER FOR ATMOSPHERIC RESEARCH
BOULDER, COLORADO

FIGURE II-11

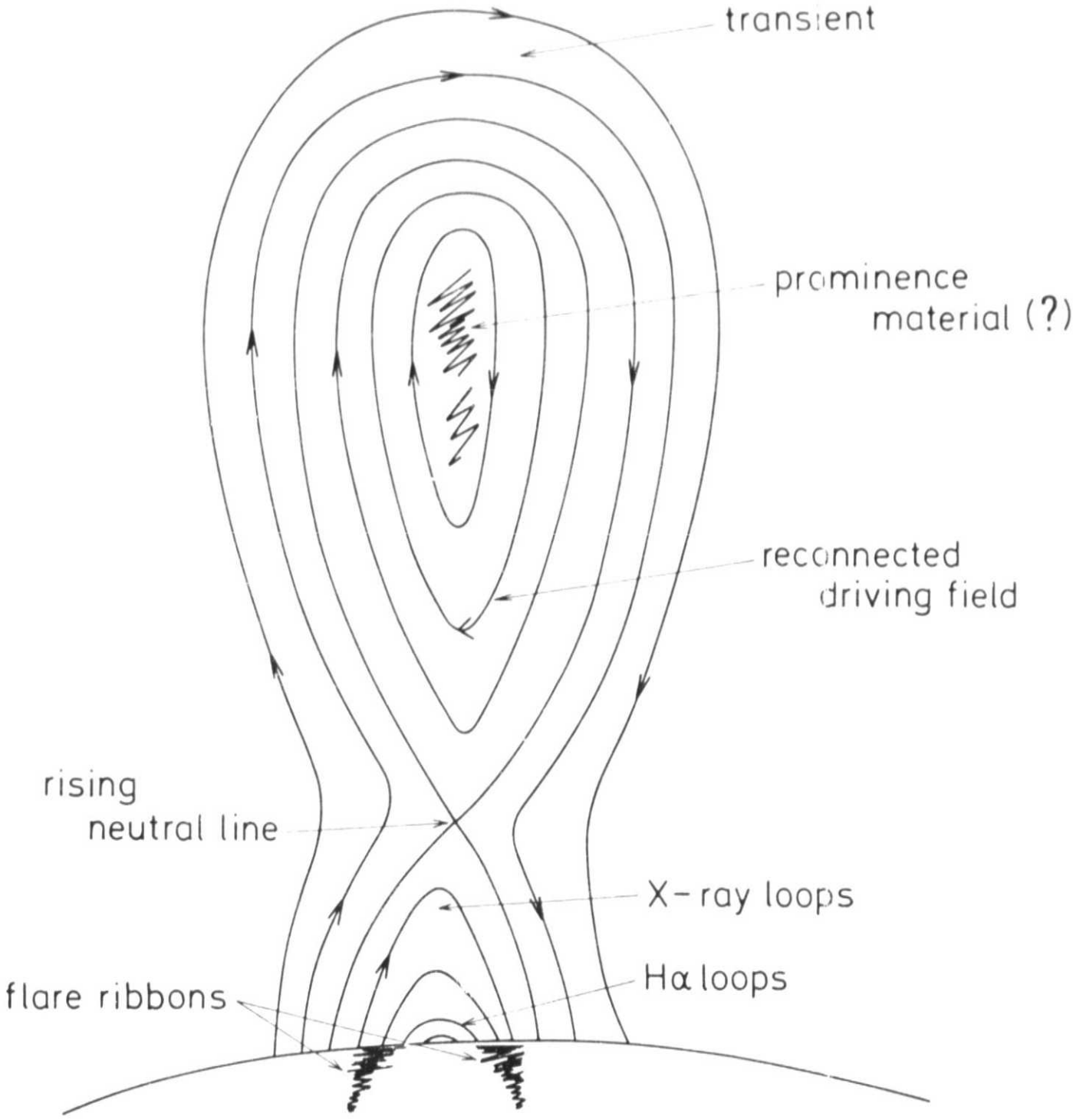
transient
prominence
material (?)
reconnected
driving field
rising
neutral line
X-ray loops
Hα loops
flare ribbons

FIGURE II-12

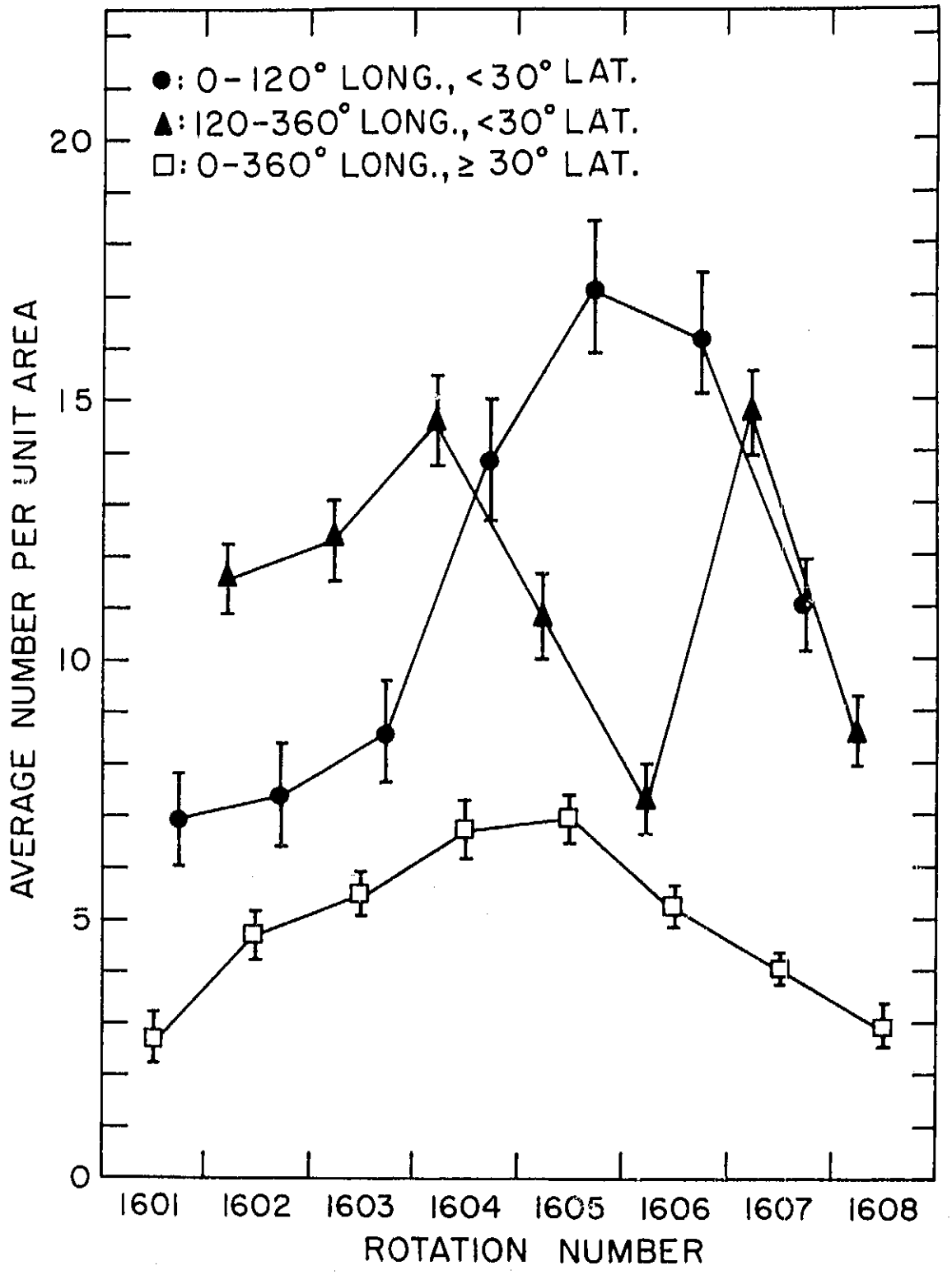
●: 0-120° LONG., <30° LAT.
▲: 120-360° LONG., <30° LAT.
□: 0-360° LONG., ≥ 30° LAT.
AVERAGE NUMBER PER UNIT AREA
0
5
10
15
20
1601
1602
1603
1604
1605
1606
1607
1608
ROTATION NUMBER

FIGURE II-13

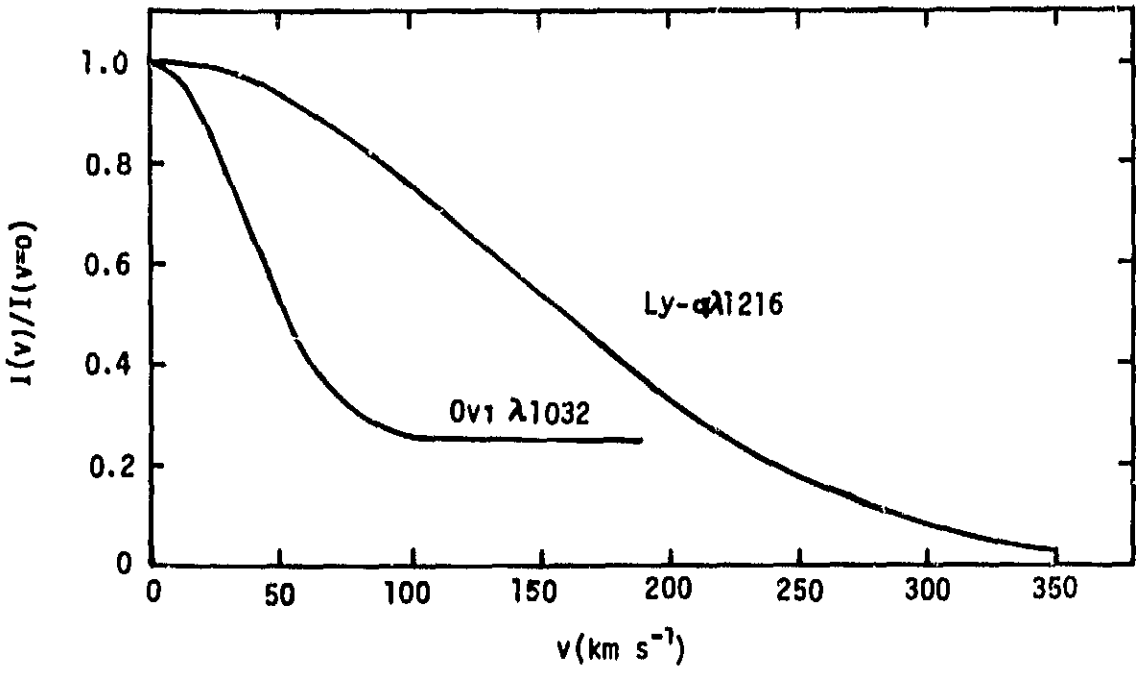

FIGURE II-14

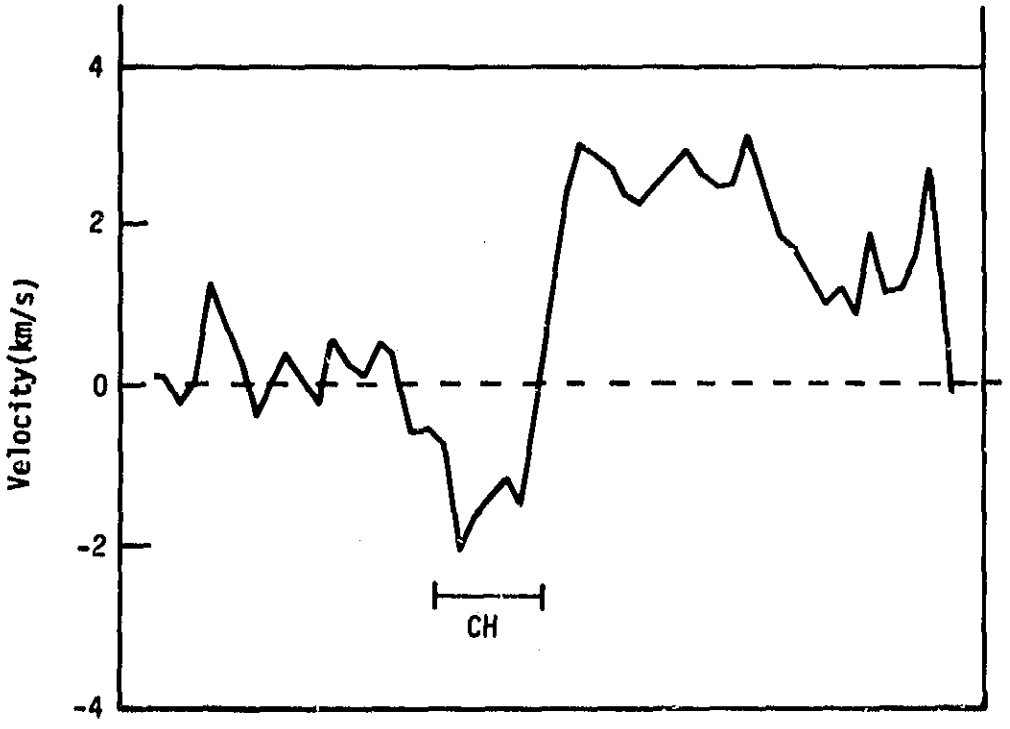

FIGURE II-15

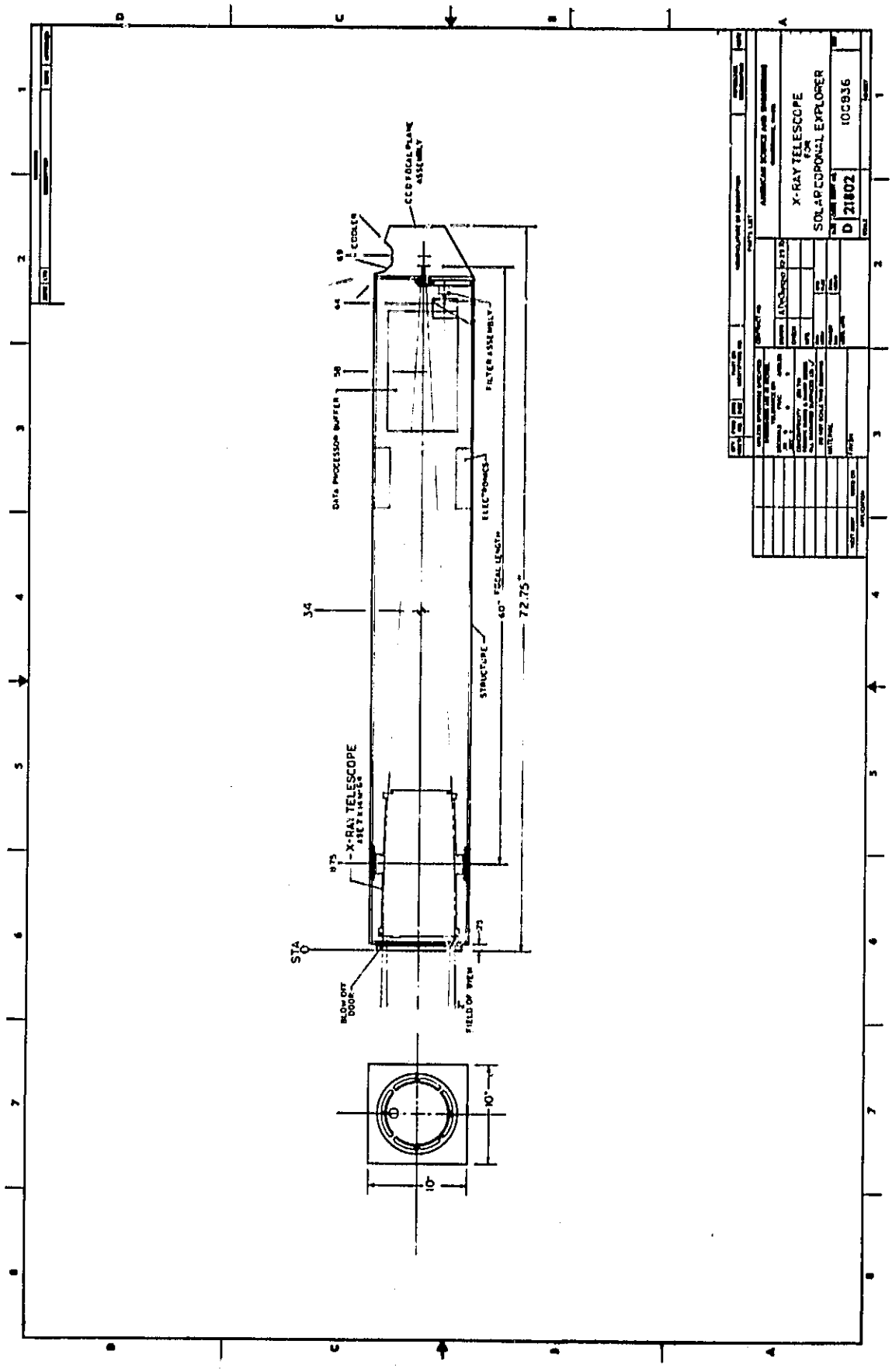
X-RAY TELESCOPE
FOR
SOLAR CORONAL EXPLORER
D 21802
100936
72.75"
60" FOCAL LENGTH
X-RAY TELESCOPE
STA 0
34
10"
16

FIGURE III - 1

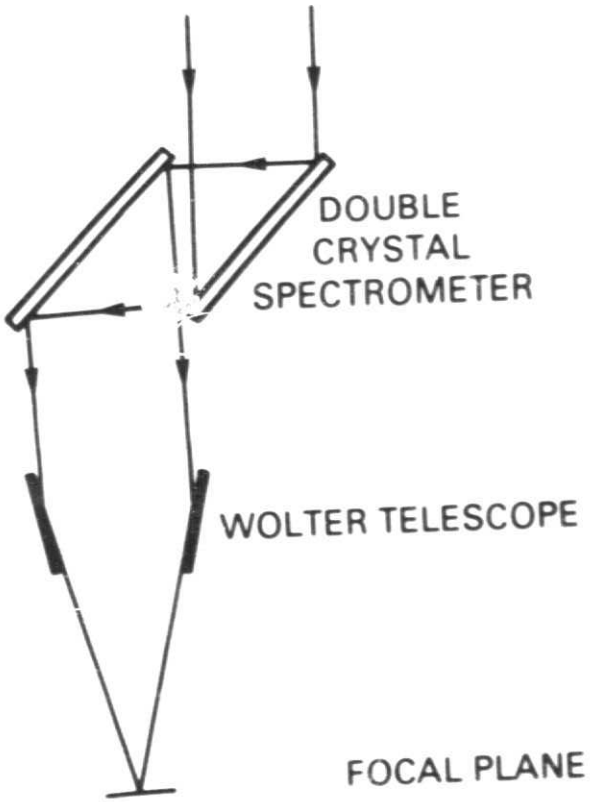

PRINCIPLE OF OBJECTIVE
CRYSTAL SPECTROMETER

FIGURE III-2a

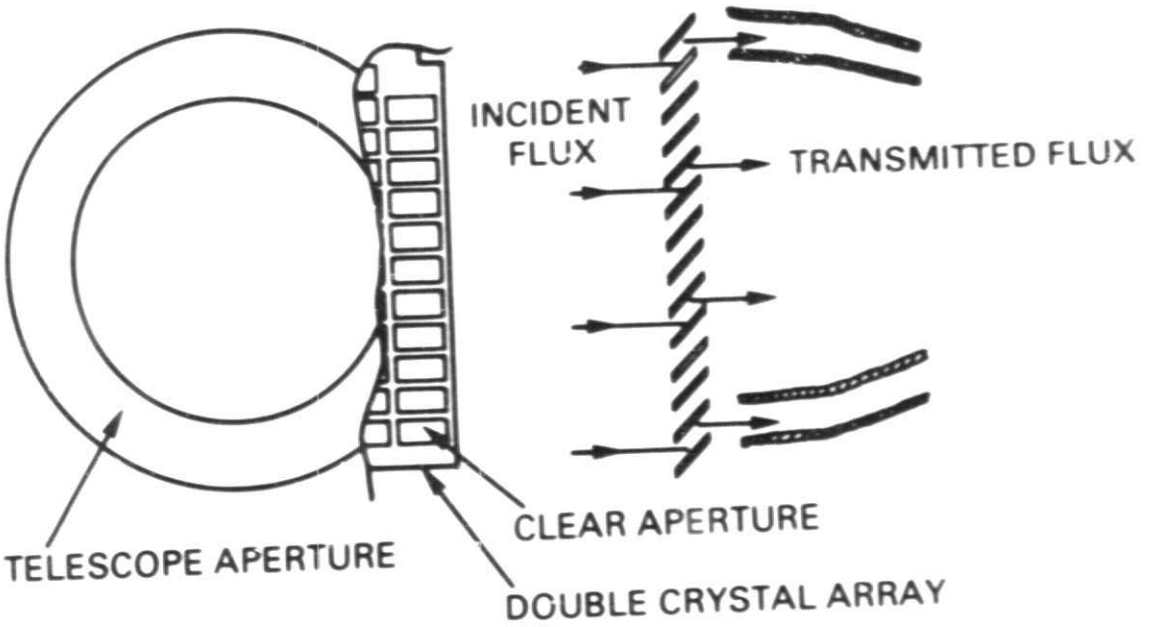

CONFIGURATION OF FLIGHT
INSTRUMENT

FIGURE III-2b

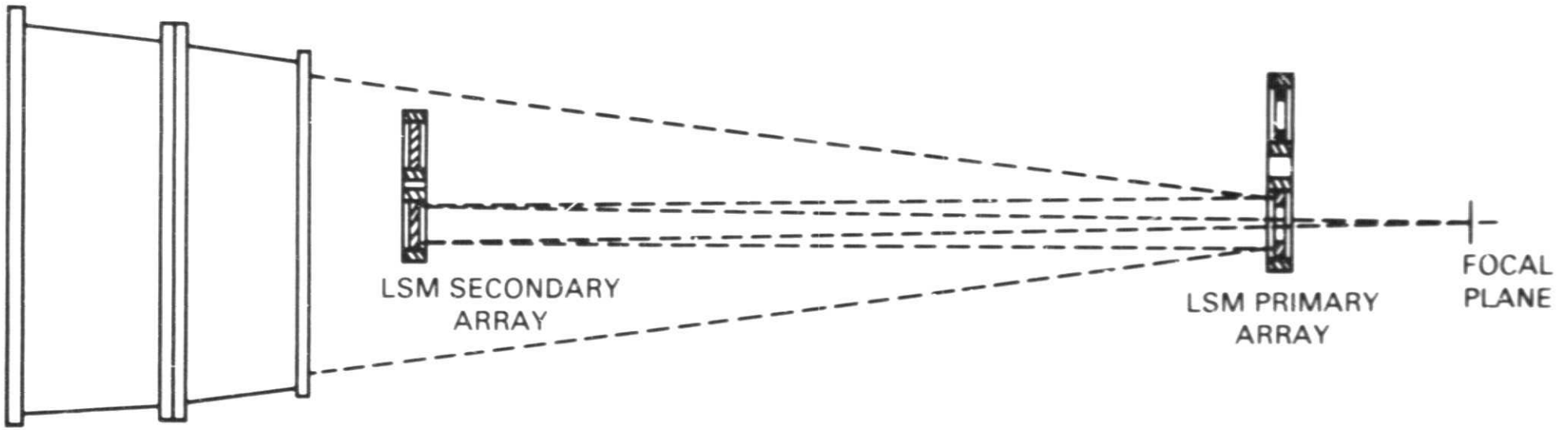

CONFIGURATION OF LSM OPTICS

FIGURE III - 2c

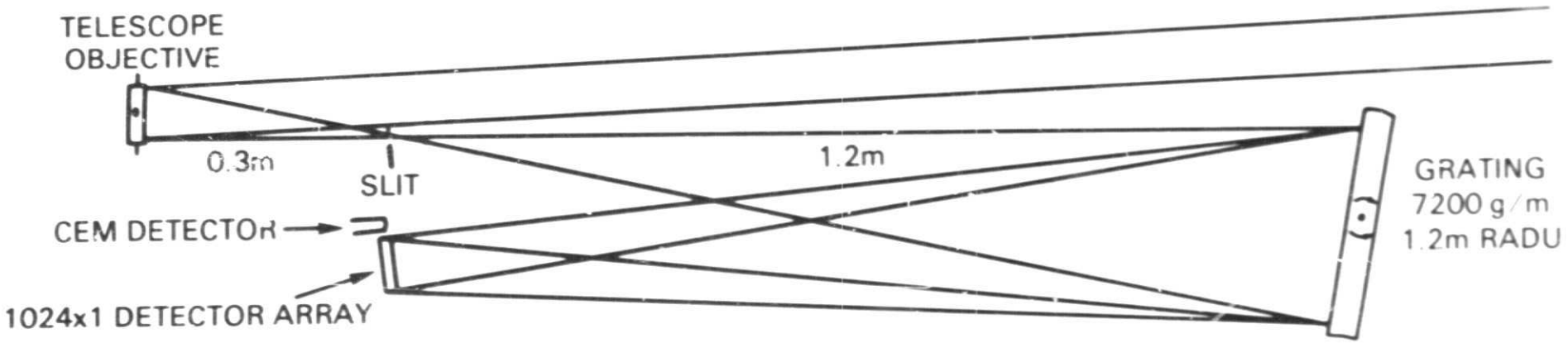

STRAWMAN EUV DIAGNOSTIC SPECTROMETER FOR THE SCE

FIGURE III - 3